
Article:
Chan, Yuk-Chun, Evans, Mathew J. orcid.org/0000-0003-4775-032X, He, Pengzhen et al. (10 more authors) (2021) Heterogeneous Nitrate Production Mechanisms in Intense Haze Events in the North China Plain. Journal of Geophysical Research: Atmospheres. e2021JD034688. ISSN 2169-8996

https://doi.org/10.1029/2021JD034688

Heterogeneous nitrate production mechanisms in intense haze events in the North China Plain

Yuk-Chun Chan[1], Mathew J. Evans[2,3], Pengzhen He[4], Christopher D. Holmes[5], Lyatt Jaeglé[1], Prasad Kasibhatla[6], Xue-Yan Liu[7], Tomás Sherwen[2,3], Joel A. Thornton[1], Xuan Wang[8], Zhouqing Xie[9], Shuting Zhai[1], and Becky Alexander[1]

[1]Department of Atmospheric Sciences, University of Washington, Seattle, WA 98195, USA

[2]National Centre for Atmospheric Science, University of York, York, YO10 5DD, UK

[3]Wolfson Atmospheric Chemistry Laboratories, Department of Chemistry, University of York, York, YO10 5DD, UK

[4]School of Environment and Tourism, West Anhui University, Lu'an, Anhui 237012, China

[5]Department of Earth, Ocean and Atmospheric Science, Florida State University, Tallahassee, FL 32306, USA

[6]Nicholas School of the Environment, Duke University, Durham, NC 27708, USA

[7]School of Earth System Science, Tianjin University, Tianjin, China

[8]School of Energy and Environment, City University of Hong Kong, Hong Kong SAR, China

[9]Anhui Key Laboratory of Polar Environment and Global Change, Department of Environmental Science and Engineering, University of Science and Technology of China, Hefei, Anhui, 230026, China

Corresponding author: Becky Alexander (beckya@uw.edu)

Key Points:

- Wintertime observations of ^{17}O excess of nitrate in Beijing suggest that the heterogeneous chemistry of NO_2 is a weak source of nitrate in intense haze.
- Ozone strongly modulates nitrate production during intense wintertime haze events in Beijing via the heterogeneous chemistry of N_2O_5.

Abstract

Studies of wintertime air quality in the North China Plain (NCP) show that particulate-nitrate pollution persists despite rapid reduction in NO_x emissions. This intriguing NO_x-nitrate relationship may originate from non-linear nitrate-formation chemistry, but it is unclear which feedback mechanisms dominate in NCP. In this study, we re-interpret the wintertime observations of ^{17}O excess of nitrate ($\Delta^{17}O(NO_3^-)$) in Beijing using the GEOS-Chem (GC) chemical transport model to estimate the importance of various nitrate-production pathways and how their contributions change with the intensity of haze events. We also analyze the relationships between other metrics of NO_y chemistry and $[PM_{2.5}]$ in observations and model simulations. We find that the model on average has a negative bias of – 0.9 ‰ and − 36% for $\Delta^{17}O(NO_3^-)$ and $[O_{x,major}]$(≡ $[O_3]$ + $[NO_2]$ + $[p\text{-}NO_3^-]$), respectively, while overestimating the nitrogen oxidation ratio ($[NO_3^-]/([NO_3^-]+ [NO_2])$) by +0.12 in intense haze. The discrepancies become larger in more intense haze. We attribute the model biases to an overestimate of NO_2-uptake on aerosols and an underestimate in wintertime O_3 concentrations. Our findings highlight a need to address uncertainties related to heterogeneous chemistry of NO_2 in air-quality models. The combined assessment of observations and model results suggest that N_2O_5 uptake in aerosols and clouds is the dominant nitrate-production pathway in wintertime Beijing, but its rate is limited by ozone under high-NO_x-high-$PM_{2.5}$ conditions. Nitrate production rates may continue to increase as long as $[O_3]$ increases despite reduction in $[NO_x]$, creating a negative feedback that reduces the effectiveness of air pollution mitigation.

Plain Language Summary

Nitrate, a major component of particles in urban air, has been identified as an important driver for recent trends in wintertime haze in the North China Plain. While it has long been known that many chemical reactions can convert gas-phase nitrogen oxides into particulate nitrate in the atmosphere, the contribution from different reactions in intense haze remains elusive. Recently, analysis of oxygen stable isotopes (^{16}O, ^{17}O, ^{18}O) in nitrate has become a promising tool for understanding its chemical origins. In this study, we re-examine the isotopic observations of nitrate in wintertime Beijing and compare them with predictions made by an air-quality model. Our analysis of observations suggests that the model likely overestimates nitrate production via the reactions between nitrogen dioxide gas (NO_2) and particles during intense haze events. After removing this nitrate formation pathway in the model, we demonstrate that nitrate production during intense haze events in Beijing is strongly modulated by ozone, a secondary pollutant whose formation is dependent on nitrogen oxides and volatile organic compounds (VOCs). Policies that result in a reduction of ozone concentrations, possibly through reductions in VOC emissions, will also reduce the formation of nitrate during wintertime haze events.

1 Introduction

Haze events, which are episodes of high concentrations of particulate matter (PM) in the lower troposphere, are common in many metropolitan areas around the world. Industrial activities, heavy traffic, and weak ventilation all favor the occurrence of haze events near population centers. The North China Plain, in particular, has been affected by intense wintertime haze in recent decades (An et al., 2019; Y.-L. Zhang & Cao, 2015). Frequent outbreaks of haze events can lead to short-term surges in premature mortality and long-term reduction in life expectancy (Y. Chen et al., 2013; Lelieveld et al., 2015; C. Song et al., 2017). An important source of fine-mode PM ($PM_{2.5}$, particulate matter with an aerodynamic diameter of equal to or less than 2.5 μm) during haze events is chemical reactions that oxidize gas-phase pollutants into $PM_{2.5}$. To mitigate haze events in metropolitan areas effectively, we must understand the chemical mechanisms driving this secondary production of $PM_{2.5}$.

Nitrate is becoming the dominant inorganic component of $PM_{2.5}$ over China in recent years, especially during wintertime haze events (Fu et al., 2020; Itahashi et al., 2018; H. Li et al., 2019; Y. Sun et al., 2020; Xu et al., 2019; Zhou et al., 2019). The Chinese government implemented a series of clean air policies since the year 2010 that imposed stricter controls on the emissions of SO_2, NO_x ($NO+NO_2$), and primary PM (Zheng et al., 2018). As a result, wintertime sulfate concentration decreased substantially by about 60% from 2014 to 2017 (H. Li et al., 2019; Zhou et al., 2019). A similar long-term concentration reduction was not observed in particulate nitrate ($p\text{-}NO_3^-$) despite a steady decline in NO_x emission in the 2010s (Fu et al., 2020; Itahashi et al., 2018; H. Li et al., 2019; Xu et al., 2019). Analysis of the aerosol sampled in Beijing in 2017 showed that nitrate contributes 25-35% to fine-mode-PM mass during wintertime haze events (H. Li et al., 2019; Xu et al., 2019), which is higher than similar observations in 2014 (<20%) (H. Li et al., 2019). In the eastern US and northern China, the concentration of wintertime secondary aerosol, including nitrate and sulfate, also responds weakly to the reduction of NO_x and SO_2 emissions, which is largely attributed to non-linear chemical feedbacks (Huang et al., 2021; Le et al., 2020; Leung et al., 2020; Shah et al., 2018; Y. Sun et al., 2020). In light of the emerging importance of nitrate in PM pollution in the North China Plain, it is essential to understand the chemistry of nitrate production during wintertime haze events in order to implement effective air pollution mitigation strategies.

Reactions of reactive nitrogen oxides ($NO_y \equiv NO_x + NO_3 + 2\times$dinitrogen pentoxide ($N_2O_5$) + nitryl chloride ($ClNO_2$) + gas-phase nitric acid (HNO_3) + particulate nitrate ($p\text{-}NO_3^-$) + nitrous acid (HONO) + halogen nitrates (ξNO_3, where ξ = Br, Cl, or I) + peroxynitric acid (HNO_4) + peroxyacylnitrates (PANs) + other organic nitrates ($RONO_2$)) control both nitrate production and oxidant budgets in the North China Plain (See Figure 1 and Table S1). Production of NO_3^- (total nitrate $NO_3^- = HNO_3 + p\text{-}NO_3^-$) is the main sink of NO_x in polluted urban air (Kenagy et al., 2018; Shah et al., 2020). In Beijing, the majority of locally produced HNO_3 quickly converts into $p\text{-}NO_3^-$ via thermodynamically controlled gas-particle partitioning (Ding et al., 2019). The dominant chemical pathway for nitrate production varies diurnally and seasonally. During the daytime, the oxidation of NO_2 by hydroxyl radical (OH) (Figure 1b, R4) dominates nitrate production, whereas the reactions of nitrate radical (NO_3) (Figure 1b, R8-12), including N_2O_5 uptake (Figure 1b, R10-11), dominate at night (Alexander et al., 2020). Shah et al. (2020) showed that N_2O_5 uptake and OH oxidation contribute similarly to NO_x loss (33% vs. 43% in

2017) over summertime in central-eastern China, which is similar to the global annual average (41-42% vs. 28-41%) (Alexander et al., 2020). In winter, on the contrary, N_2O_5 uptake dominates over OH oxidation (51% vs. 23%) (Shah et al., 2020). The conversion of NO_x to NO_3^- is coupled to many other reactive species in the atmosphere, including ozone, peroxy radicals (RO_2), and HONO. For instance, the production of NO_3 radical requires ozone (Figure 1b, R6); yet the efficiency of ozone production is, in turn, controlled by the amount of NO_x and peroxy radicals. Meanwhile, the uptake of NO_2 on aerosols (Figure 1b, R5) and photolysis of p-NO_3^- can produce HONO, which yields OH readily upon photolysis and may control the tropospheric oxidizing capacity during haze events (L. Li et al., 2018; Z. Tan et al., 2019; J. Zhang et al., 2019). A comprehensive representation of nitrate chemistry in models is necessary for accurate predictions of air quality in winter.

While heterogeneous chemistry (i.e., multi-phase reactions) of NO_y is critical to wintertime nitrate production in urban air, its complexity represents a major source of uncertainty in many air-quality models. The uptake of NO_2 on aerosols, which has been presumed to be a sink of NO_x and a source of NO_3^- and HONO in models, was re-examined in recent modeling studies. Holmes et al. (2019) decreased the uptake coefficients of NO_2 ($\gamma(NO_2)$) in their model after considering the lower estimates of $\gamma(NO_2)$ reported in more recent laboratory studies. Jaeglé et al. (2018) showed that changing the HONO yield of NO_2 uptake to 100% (no HNO_3 formation) improves the simulation of NO_y chemistry over wintertime Northeast United States. A global model study by Alexander et al. (2020) demonstrated that NO_2 uptake has the largest potential influence over the North China Plain. For N_2O_5 uptake on aerosol, the efficiency of nitrate formation is sensitive to the chemical composition (e.g., [Cl^-], [p-NO_3^-], and thickness of organic coating), pH, and water content of aerosols (Bertram & Thornton, 2009; Gaston et al., 2014; Tham et al., 2016; Xia et al., 2019; Zhou et al., 2018). Laboratory-based predictions of the uptake coefficient of N_2O_5 ($\gamma(N_2O_5)$) on aerosols often differ from the observation-based estimates by orders of magnitudes (e.g., McDuffie et al., 2018; C. Yu et al., 2020). In addition to reactions on aerosol surfaces, recent modeling studies also suggest that uptake of NO_y in cloud droplets is an overlooked sink of NO_x (Holmes et al., 2019). Cloud uptake of NO_y contributes up to 25% NO_x loss at higher latitudes annually (Alexander et al., 2020; Holmes et al., 2019). Given the large number of remaining uncertainties in heterogeneous chemistry of NO_y, models need additional observational constraints for improving the representation of these chemical processes in air quality models.

The oxygen isotopic composition of nitrate provides an independent piece of information related to the formation of nitrate. In particular, ^{17}O excess ($\Delta^{17}O$) in nitrate, which is determined solely by the relative importance of ozone to other oxidants during the oxidation of the members of NO_y family (Michalski et al., 2003), has proven to be a promising proxy for quantifying nitrate-production mechanisms in various environmental contexts (e.g., Alexander et al., 2020; Geng et al., 2017; Savarino et al., 2013). Shao et al. (2019) analyzed observations of $\Delta^{17}O(SO_4^{2-})$ in wintertime Beijing and demonstrated the importance of heterogeneous chemistry for sulfate formation during haze events. For $\Delta^{17}O(NO_3^-)$, three previous studies have reported observations in the North China Plain during winter haze events (He et al., 2018; W. Song et al., 2020; Y. Wang et al., 2019). Their analyses of the observations suggested that uptake of N_2O_5 and the oxidation of volatile organic compounds (VOCs) by NO_3 radicals (Figure 1b, R12) dominate wintertime nitrate production near Beijing. However, their interpretation of the observations

157 relies on highly simplified models of nitrate production and several assumptions about the
158 concentration of radicals in urban air. In this study, we use a 3-D chemical transport model with
159 coupled HO_x-NO_x-VOC-ozone-halogen-aerosol tropospheric chemistry to re-interpret the
160 observations of $\Delta^{17}O(NO_3^-)$ in the North China Plain in order to gain insight into the
161 mechanisms of NO_y chemistry during winter haze events.
162
163

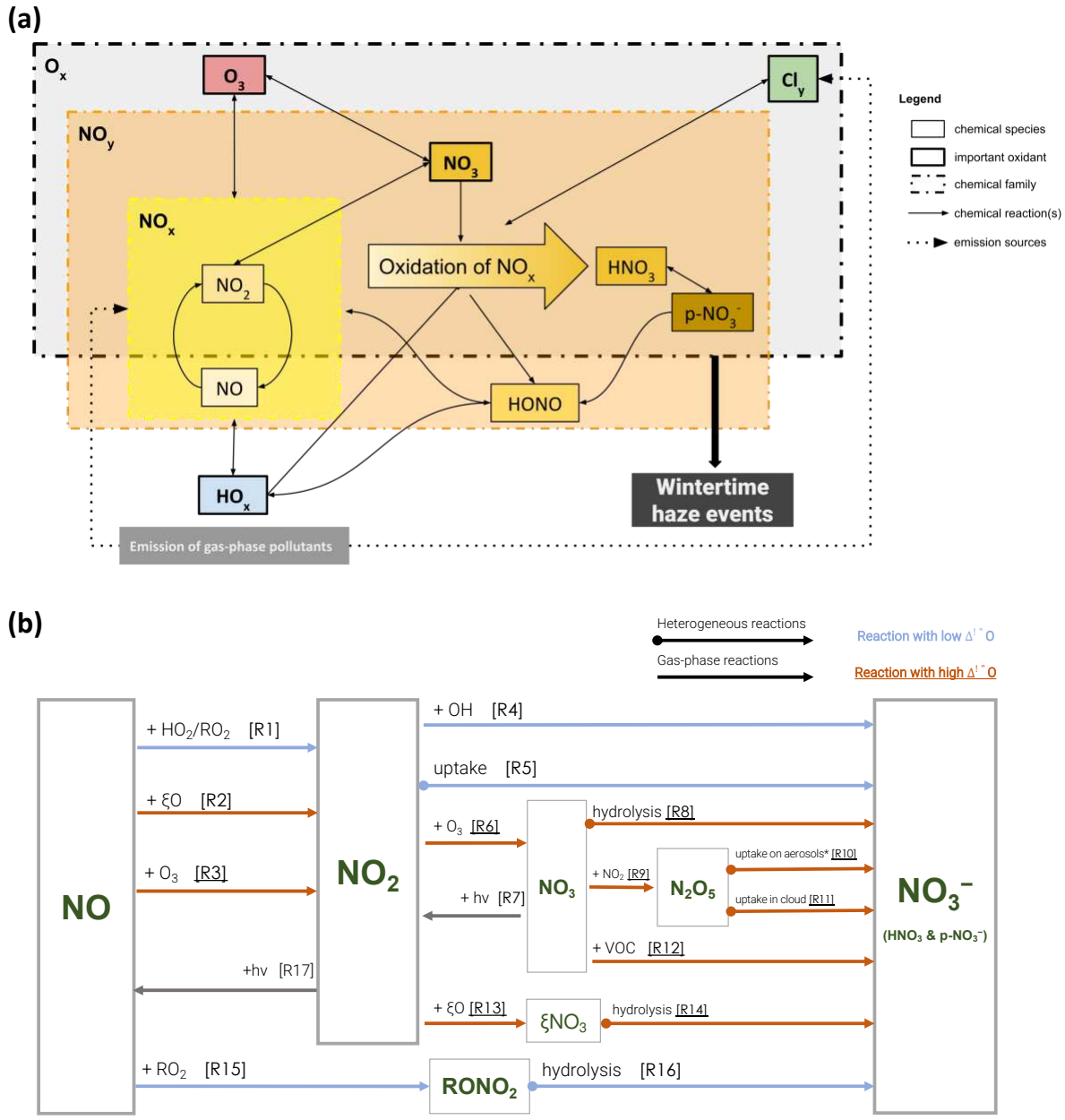

Figure 1. Simplified schematic of the chemistry of nitrate production in urban air. 1(a) is the schematic of the coupling of nitrate production and the emission of gas-phase pollutants, the NO_y chemical family, the budget of odd oxygen species, and PM pollution. 1(b) is the schematic of nitrate production pathways in the model and important intermediate species from the oxidation of NO_x to NO_3^- ($[NO_3^-] = [HNO_3] + [p\text{-}NO_3^-]$). "ξ" stands for the

halogens (Cl/ Br/I), while "VOC" stands for volatile organic compounds. N_2O_5 uptake on aerosols (R10) can undergo two possible pathways, depending on the chloride content in the aerosol. The chemical equation and other details of the reactions R1 to R17 can be found in Table S1.

164

2 Data and Methods

2.1 Measurements of $\Delta^{17}O(NO_3^-)$, aerosol, and trace gases during Beijing in winter 2014-15

Observations of $\Delta^{17}O(NO_3^-)$ in Beijing were previously published in He et al. (2018), Y. Wang et al. (2019), and W. Song et al. (2020) and are briefly described here. Most of the aerosol samples were collected in the Beijing metropolitan area from October 2014 to January 2015 and later sent to IsoLab at the University of Washington for isotopic analysis. The location of the measurement sites is shown in Figure S1(a). He et al. (2018) and W. Song et al. (2020) used collection intervals of about 12 hours for each aerosol sample, whereas Y. Wang et al. (2019) used 23 hours. The aerosol filters collected both HNO_3 and p-NO_3^-, so the observed $\Delta^{17}O(NO_3^-)$ contains $\Delta^{17}O$ signals from both species (He et al., 2018). We compute the daily mean of $\Delta^{17}O(NO_3^-)$ from these published measurements and obtain a dataset with 51 data points between 1 October 2014 and 15 January 2015.

To evaluate the modeled concentration of $PM_{2.5}$, p-NO_3^-, NO_2, and ozone in Beijing, we use measurements of these species reported in He et al. (2018), Y. Wang et al. (2019), and W. Song et al. (2020). We also consider similar measurements at other Beijing air-quality stations that are operated by the China Ministry of Ecology and Environment as a complementary dataset (location of these sites are shown in Figure S1(a)). These air-quality measurements are publicly available on https://quotsoft.net/air (last accessed on 26 January 2021).

2.2 GEOS-Chem 3-D Chemical Transport Model simulations

We use the three-dimensional global chemical transport model GEOS-Chem (version 12.7.0; hereafter GC) to simulate the evolution of haze events in winter 2014-15. This version of the GC model code is accessible from https://doi.org/10.5281/zenodo.3634864 (last accessed on 26 January 2021). The model considers detailed HO_x-NO_x-VOC-ozone-halogen-aerosol chemistry in the troposphere (Fisher et al., 2018; Kasibhatla et al., 2018; Sherwen et al., 2017; X. Wang et al., 2019, 2020). The Fast-JX module in GC calculates aerosol radiative effects and photolysis rates (Eastham et al., 2014; Neu et al., 2007). The partitioning between the HNO_3 and p-NO_3^- is determined by an aerosol thermodynamic equilibrium module ISORROPIA II (Fountoukis & Nenes, 2007). The deposition schemes for trace gases and aerosols in GC are described in Y. Wang et al. (1998), H. Liu et al. (2001), L. Zhang et al. (2001), and Jaeglé et al. (2018). Since GC uses offline meteorological data to drive simulations by design, it will not be able to capture the feedback processes involving aerosol-boundary interaction, which can potentially be important during haze events in wintertime East China (Huang et al., 2020). Earlier versions of GC have also been used to investigate NO_x and PM pollution in metropolitan areas (e.g., Jaeglé et al., 2018; Shah et al., 2020).

The NO_y chemistry in GC has been updated substantially in recent versions of the model. Holmes et al. (2019) modified the uptake coefficients for NO_2, NO_3, and N_2O_5 on different aerosols based on recent laboratory studies. In particular, $\gamma(NO_2)$ on sulfate-nitrate-ammonium (SNA) aerosol has been set to 5×10^{-6}, which is a factor-of-20 reduction compared to the previous work. The latest versions of GC also incorporated the uptake of NO_2, NO_3 and N_2O_5 in

cloud droplets, following the entrainment-limited scheme described in Holmes et al. (2019) for partly cloudy conditions. For the uptake of N_2O_5 on SNA aerosol, the latest version of GC now considers the inhibiting effects of organic coating through the parametrization described in McDuffie et al. (2018), which was built on top of the Bertram and Thornton (2009) scheme to calculate the reaction probability of N_2O_5 on aerosol. Particulate-nitrate photolysis described in Kasibhatla et al. (2018) is currently an optional feature in GC and is switched off by default. For gas-phase NO_y chemistry, the latest updates include the reactions of C1-C3 alkyl nitrate, as described in Fisher et al. (2018). While the previous studies independently showed that these chemistry updates improved the representation of NO_y in the model, no study to date has yet examined the combined effects of these updates on model simulations of wintertime haze events in China.

In this study, we use version 12.7.0 of GC as our "base model". Driven by GEOS-FP meteorological data assimilation products with a native horizontal resolution of 0.25° x 0.3125° and 72 vertical levels, the base simulation was run at a coarser spatial resolution (4° latitude x 5° longitude and 47 vertical levels) to attain global coverage. We also performed nested-grid regional simulations for East Asia at a higher horizontal resolution (0.25° latitude x 0.3125° longitude) by using output from the corresponding global simulations as boundary conditions (See Figure S1(b) and S1(c) for grid size and boundaries). The model simulates the mixing of chemical species in the planetary boundary layer using the non-local mixing scheme from Lin and McElroy (2010). Anthropogenic emissions of reactive gases and aerosols over the United States, Canada, Asia, and Africa are from the regional emissions inventories EPA/NEI2011, APEI, MIX, and DICE-Africa, respectively (M. Li et al., 2017; Marais & Wiedinmyer, 2016). NO_x emissions from MEIC (the emission inventory for China in MIX framework) between 2005 and 2018 have recently been validated by the satellite retrievals of NO_2 columns in Shah et al. (2020) and showed a good agreement. Emissions in the rest of the world are from the Community Emissions Data System (CEDS) inventory (Hoesly et al., 2018). Biomass burning emissions are from the Global Fire Emissions Database (GFED 4.1s) (van der Werf et al., 2017). Lightning-NO_x emissions in the model are estimated based on a satellite lightning climatology described in Murray et al. (2012). Soil-NO_x emissions are estimated offline using the algorithm described in Hudman et al. (2012). The model simulation period is from August 2014 to January 2015, in which the first two months are used for "spinning-up" the model. To address the uncertainty in NO_y chemistry, we conduct a series of model sensitivity experiments at 4° latitude x 5° longitude resolution. The detailed configurations for these simulations are described in Section 3.2.2 and Text S2 in SI.

2.3 Calculation of $\Delta^{17}O(NO_3^-)$ in model simulations

Following the approach of Alexander et al. (2020), we use local chemical production rates to calculate $\Delta^{17}O(NO_3^-)$, by which we assume that $\Delta^{17}O(NO_3^-)$ is controlled by local NO_x cycling and nitrate production (See Figure S2). This method works well for intense haze events in wintertime North China Plain, where most NO_3^- is produced locally over the North China Plain (See Figure S3). The $\Delta^{17}O$ in tropospheric ozone ($\Delta^{17}O(O_3)$) is assumed to be 26‰ based on recent measurements (Vicars & Savarino, 2014). We assume that only the terminal oxygen atom of ozone is transferred during oxidation reactions; hence the $\Delta^{17}O$ value of the oxygen atom

transferred is equal to 39‰ ($= \frac{3}{2} \times 26‰$, denoted as $\Delta^{17}O(O_3^*)$) (Morin et al., 2011). For calculation of $\Delta^{17}O(NO_2)$, we assume isotopic equilibration during the daytime for all nitrate production pathways. The longer lifetime of NO_x in wintertime North China Plain (≈ 21 to 27 hours estimated by Shah et al. (2020)) suggests that NO_x oxidation rates are slow enough to make this a reasonable assumption. Figure S2 also shows the assumed $\Delta^{17}O(NO_3^-)$ values for each nitrate formation pathway in the model.

2.4 Other metrics for evaluating NO_y chemistry

In addition to $\Delta^{17}O$, we also use the concentration and speciation of the odd oxygen family (O_x) to evaluate the performance of the model in simulating NO_y chemistry. In theory, O_x includes all the chemical species that cycle with ozone and atomic oxygen in the atmosphere via photochemical reactions and is highly coupled with the local nitrate production (Bates & Jacob, 2020; Lu et al., 2019; Womack et al., 2019).

Here, we define total O_x as the weighted sum of ozone and other species that cycle with ozone and atomic oxygen in the model:

$$O_x \equiv O_3 + NO_2 + 2NO_3 + 3N_2O_5 + HNO_3 + \text{p-}NO_3^- + PANs + RONO_2 + HNO_4 + \xi O + \xi NO_2 + 2\xi NO_3 + \sum_{n=2}^{5} n\xi_2O_n + 2O\xi O$$

where ξ = Br, Cl, or I. Our definition of O_x is very similar to the one used in Bates and Jacob (2020), except that we (1) include p-NO_3^- and (2) exclude the short-lived radical species (e.g., $O(^1D)$ and Criegee intermediates) that have a negligible impact on total O_x abundances. We consider p-NO_3^- to be an O_x member because of the rapid equilibrium partitioning between HNO_3 and p-NO_3^- on fine-model aerosol and the potential importance of renoxification in urban air from the photolysis of p-NO_3^- (Bao et al., 2018; Kasibhatla et al., 2018; Y. Liu et al., 2019; Ye et al., 2017). Womack et al. (2019) also included p-NO_3^- in their definition of generalized odd oxygen family. While GC can simulate and output all the species listed in our definition of O_x, most of the measurements in Beijing only include the concentration of O_3, NO_2, and p-NO_3^- (with possible interference of HNO_3, as explained in Section 2.1). The incomplete observations of O_x only have minor effects on our model-observation comparison because O_3, NO_2, and p-NO_3^- are the dominant (>95%) O_x species in wintertime Beijing in the model (See more detailed analysis in Section 3.1). We denote the sum of O_3, NO_2, and p-NO_3^- as $O_{x,major}$.

Since the speciation of O_x is sensitive to NO_y chemistry, we also compare the ratio of different O_x species in the observations and the model simulations. In particular, we compute the nitrogen oxidation ratio (NOR) using the mixing ratios of NO_2 and NO_3^-:

$$NOR \equiv \frac{[NO_3^-]}{[NO_3^-] + [NO_2]} = \frac{[\text{p-}NO_3^-] + [HNO_3]}{[\text{p-}NO_3^-] + [HNO_3] + [NO_2]}$$

NOR ranges from 0 (complete absence of NO_3^-) to 1 (complete oxidation of all NO_2). This dimensionless ratio indicates the efficiency of the oxidation of NO_x and is less prone to absolute errors in simulating NO_x concentrations (such as uncertainties in emissions). NOR has been widely used in the analysis of nitrate formation mechanisms in other studies (e.g., He et al., 2018; P. Liu et al., 2020; Shi et al., 2019; Xu et al., 2019).

2.5 Haze-regime categorization

To facilitate our analysis of the relationships between the chemistry metrics and the intensity of haze events, we categorize the data into four haze regimes according to the surface $PM_{2.5}$ concentration: "light haze" ($[PM_{2.5}] \leq 75$ μg m^{-3}), "moderate haze" events (75 μg $m^{-3} < [PM_{2.5}] \leq$ 150 μg m^{-3}), "severe haze" events (150 μg $m^{-3} < [PM_{2.5}] \leq 225$ μg m^{-3}), and "extreme haze" events ($[PM_{2.5}] > 225$ μg m^{-3}) (See Table S2 for the frequency of different haze regimes). For the observations, we compute the average of daily mean $[PM_{2.5}]$ observed at the Beijing air-quality stations (both urban and suburban stations, 22 stations in total) to determine the haze regime of a particular day. The inter-station average $[PM_{2.5}]$ can better reflect the intensity of regional haze events than the single-station measurements. For model data, we use the modeled, mean surface $[PM_{2.5}]$ over the Beijing gridbox in coarse-resolution simulations. It is noted that the choice of this categorization does not imply the existence of statistically significant differences between chemical metrics in different haze regimes or abrupt shifts in NO_y chemistry at regime boundaries (where $[PM_{2.5}] = 75$, 150, or 225 μg m^{-3}). Instead, this categorization is merely used for illustrating and communicating some general trends in NO_y chemistry as haze intensifies. Similar categorizations have also been adopted in other studies of nitrate pollution in Beijing (e.g., Fu et al., 2020; He et al., 2018; P. Liu et al., 2020). When we are referring to patterns that are seen across multiple haze regime, the terms "intense haze" ($[PM_{2.5}] > 75$ μg m^{-3}) and "more intense haze" ($[PM_{2.5}] > 150$ μg m^{-3}) are sometimes used.

3 Results

3.1 Observations of $\Delta^{17}O(NO_3^-)$ in Beijing

A compilation of all available $\Delta^{17}O(NO_3^-)$ observations reveals a positive relationship between $\Delta^{17}O(NO_3^-)$ and $PM_{2.5}$ concentration in Beijing during winter 2014-15 (Figure 2). The median of $\Delta^{17}O(NO_3^-)$ increases from 26.1‰ in light haze to 31.5‰ in extreme haze (Figure 2b). Similar positive relationships between $\Delta^{17}O(NO_3^-)$ and $[PM_{2.5}]$ have also been reported in He et al. (2018) and Y. Wang et al. (2019). The positive relationship can still be seen when we analyze daytime and nighttime measurements separately (Figure S4). The lack of strong diurnal variability in $\Delta^{17}O(NO_3^-)$ in observations is consistent with the long lifetime of NO_x in wintertime North China Plain shown by previous modeling studies (e.g., Shah et al., 2020). The higher $\Delta^{17}O(NO_3^-)$ measured in intense haze indicates that the relative importance of high-$\Delta^{17}O$ pathways involving O_3 increases with $PM_{2.5}$ concentration.

Figure 2 also shows that the variability of $\Delta^{17}O(NO_3^-)$ is larger on days with lower $[PM_{2.5}]$. The standard deviation (s.d.) of $\Delta^{17}O(NO_3^-)$ decreases from 3.7‰ in light haze to 1.7‰ intense haze.

345 The observed smaller variability of $\Delta^{17}O(NO_3^-)$ in intense haze may be explained by the weaker
346 ventilation and the overwhelming contribution of nitrate from local production (See Figure S3).
347 We also note that very high variability in $\Delta^{17}O(NO_3^-)$ is only seen in the light-haze observations
348 from Y. Wang et al. (2019) (the corresponding s.d. is 3.9‰). Observations in He et al. (2018) and
349 W. Song et al. (2020) show a similar variability in $\Delta^{17}O$ (the overall s.d. are 1.6‰ and 1.4‰,
350 respectively) and do not contain the low $\Delta^{17}O(NO_3^-)$ values (<26‰) reported by Y. Wang et al.
351 (2019). Thus, we focus our analysis more on intense haze when the observations from all three
352 studies are in better agreement on the magnitude and variability in $\Delta^{17}O(NO_3^-)$.
353

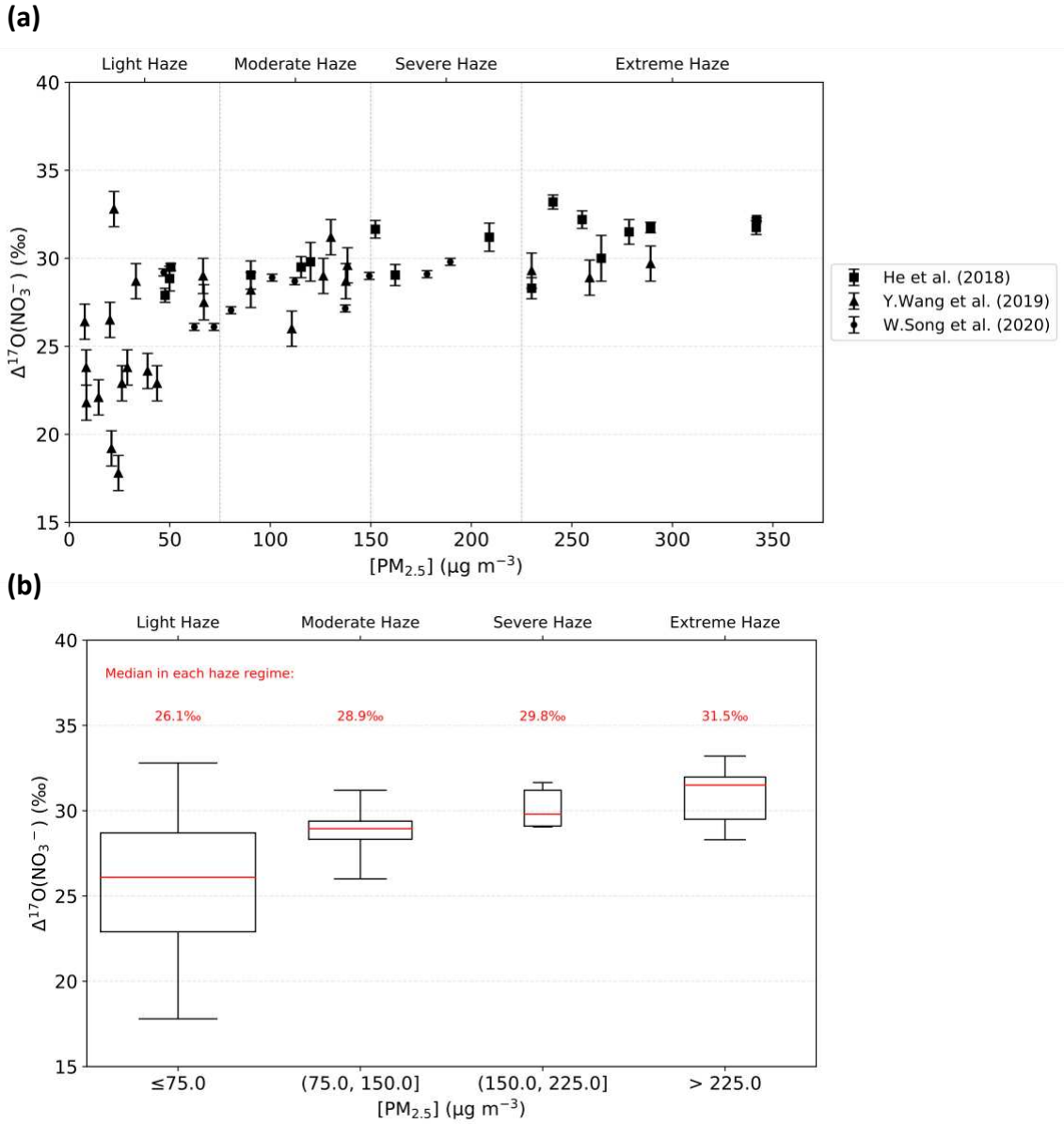

Figure 2. Observed relationship between $\Delta^{17}O(NO_3^-)$ and $PM_{2.5}$ concentration. The scatter plot in 2(a) shows the daily-average measurements in He et al. (2018) (squares), Y. Wang et al. (2019) (triangles), and W. Song et al. (2020) (circles). The number in red above each box shows the value of the median of $\Delta^{17}O(NO_3^-)$ in each haze regime. The error bars

represent the ± 2σ standard deviation uncertainty range for the $\Delta^{17}O$ measurements. The box plot in 2(b) shows the statistics of the observed $\Delta^{17}O(NO_3^-)$ in each haze regime. The red line indicates the median; the top and the bottom of the box indicate the 75th percentile and the 25th percentile, respectively; the whiskers indicate the maximum and the minimum. The width of boxes scales with the number of samples in each haze regime.

3.2 Model Results

3.2.1 Base Model

Figure 3 compares the magnitude of modeled and observed $\Delta^{17}O(NO_3^-)$ in Beijing in intense haze. While the modeled median $\Delta^{17}O(NO_3^-)$ in moderate haze (29.5‰) and severe haze (29.1‰) lie within the range of observations, most of the modeled $\Delta^{17}O(NO_3^-)$ in extreme haze (median = 27.3‰) are lower than the minimum value in the observations (28.3‰). The lower $\Delta^{17}O(NO_3^-)$ in extreme haze compared to moderate and severe haze means the base model predicts a negative relationship between $\Delta^{17}O(NO_3^-)$ and $[PM_{2.5}]$ in intense haze (Figure 3), which is the opposite relationship shown in the observations. Modeled median $\Delta^{17}O(NO_3^-)$ in moderate haze is 2.2‰ higher than that in extreme haze. Lower $\Delta^{17}O(NO_3^-)$ in extreme haze cannot be explained by the modeled difference in $\Delta^{17}O(NO_2)$, of which the median changes by less than 0.5‰ across different types of haze events (Figure S5).

The base model also cannot reproduce a sufficient amount of O_x, the observed O_x speciation, nor the observed NOR in Beijing in intense haze (Figure 4 and Figure 5). Modeled $[O_{x,\,major}]$ in intense haze is 36% lower than the observations on average. The bias in modeled $[O_x]$ in the North China Plain is mainly caused by an underestimate of $[NO_2]$ and $[O_3]$ (Figure 4, and more discussion in Section 4.2). In extreme haze, the base model underestimates the mean of $[NO_2]$ and $[O_3]$ by 55% and 54%, respectively. The large model-observation discrepancy in $[NO_2]$ cannot be explained by the long-known interference of NO_z species (members in the NO_y family that are not NO or NO_2) in chemiluminescence-based measurements (Lamsal et al., 2008; Reed et al., 2016), because both our model (see Figure S6) and other observations suggest that non-NO_3^- gas-phase NO_z species' (e.g., PAN) concentration is small in comparison with $[NO_x]$ in wintertime in Beijing (S. Chen et al., 2020; B. Zhang et al., 2017; G. Zhang et al., 2020; H. Zhang et al., 2014). The underestimate of NO_2 leads to a modeled overestimate of NOR (0.33) in intense haze compared to the observations (0.21). The discrepancy between modeled and observed NOR increases with $[PM_{2.5}]$. In extreme haze, the modeled median NOR (0.50) is higher than the observed maximum (0.47) (Figure 5).

The base model's bias in $\Delta^{17}O(NO_3^-)$, $[O_x]$, and NOR persists even when a higher horizontal spatial resolution is used. The range of the chemical metrics increases with model resolution, but the median and the mean remain largely unchanged (Figures 3, 4 and 5). The relationship between modeled $\Delta^{17}O(NO_3^-)$ and $[PM_{2.5}]$ is still negative in intense haze (Figure 3). Moreover, the extended range of modeled $\Delta^{17}O(NO_3^-)$ still cannot capture the maximum and minimum in observations. A similar model underestimate of mean $[O_x]$ during intense haze events is seen in both the regional-level and the site-level comparison (Figure 4 and Figure S7). The nested-grid simulation predicts a slightly lower median NOR (− 0.01, − 0.05, and − 0.07 in moderate, severe,

and extreme haze, respectively), but the modeled NOR is still too high compared to the observations (Figure 5). The comparison between nested-grid and global simulations suggests that low horizontal spatial resolution is not the fundamental cause for the model's bias in NO_y chemistry over the North China Plain. Comparison of observed and modeled mixed layer depths also suggests that the bias in the thickness of vertical mixing layer is not a cause of the model biases in trace gas concentrations (See Figure S8).

In the base simulation, the major low-$\Delta^{17}O$ pathways in Beijing are gas-phase oxidation of NO_2 by OH and NO_2 uptake on aerosols, which contribute 34.4% and 19.0 % to nitrate production on average over winter 2014-15, respectively (Figure 6). The major high-$\Delta^{17}O$ pathways are N_2O_5 uptake on aerosols (33.6%) and clouds (11.3%) (Figure 6). The relative importance of high-$\Delta^{17}O$ pathways and low-$\Delta^{17}O$ pathways remains at around a ratio of 1:1 from light haze to severe haze events. In extreme haze, the contribution from NO_2 uptake increases sharply to 35.9% and becomes higher than N_2O_5 uptake on aerosols and clouds (30.0%), resulting in relatively low values of $\Delta^{17}O(NO_3^-)$ (Figure 6).

The model-observation comparison of the $\Delta^{17}O(NO_3^-)$ in extreme haze suggests that the standard version of GC either overestimates the contribution of low-$\Delta^{17}O$ pathways and/or underestimates the contribution of high-$\Delta^{17}O$ pathways as $PM_{2.5}$ increases. In the base simulation, the modeled reduction in $\Delta^{17}O(NO_3^-)$ in extreme haze is driven by an increase in NO_2 uptake rate and a decrease in N_2O_5 uptake on aerosols (Figure 6a), suggesting that the modeled rate of NO_2 uptake is too high and/or the rate of N_2O_5 uptake is too low in extreme haze. It is also possible that the model underestimates the contribution of the other high-$\Delta^{17}O$ nitrate production pathways, such as reactions between NO_3 and VOCs (Figure 1b, R12) and the hydrolysis of halogen nitrates (Figure 1b, R14). However, further analysis and model sensitivity simulations suggest that either these reactions are negligible and/or cannot resolve the model biases in the chemical metrics because of the limited supply of NO_3 and N_2O_5 in intense haze (Refer to Text S1 and Text S2.2 in SI).

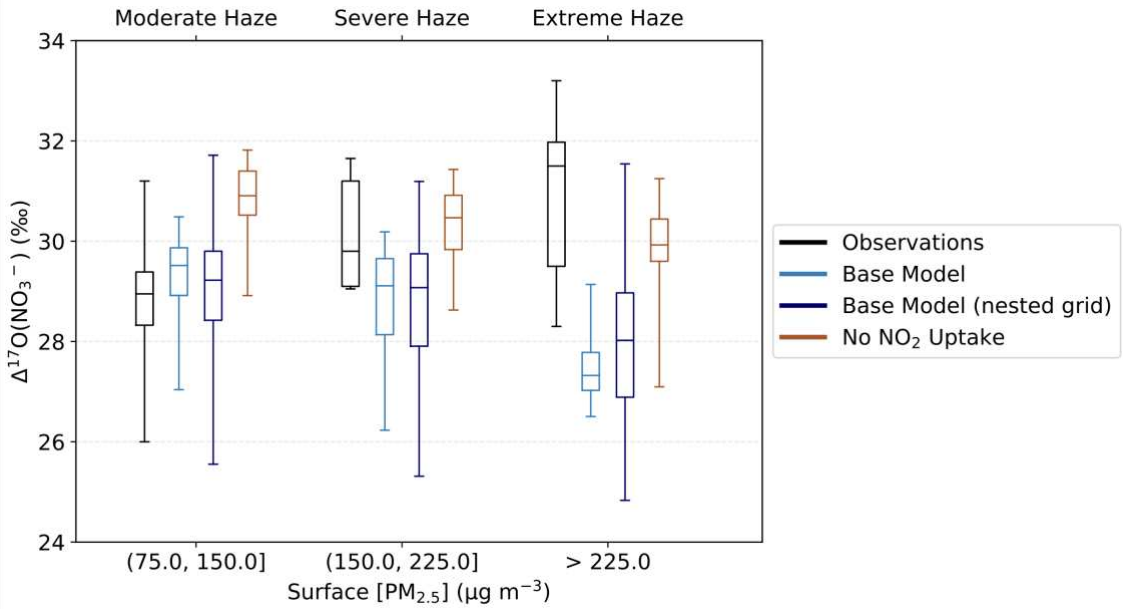

Figure 3. Comparison of $\Delta^{17}O(NO_3^-)$ in observations and model simulations under different haze regimes.

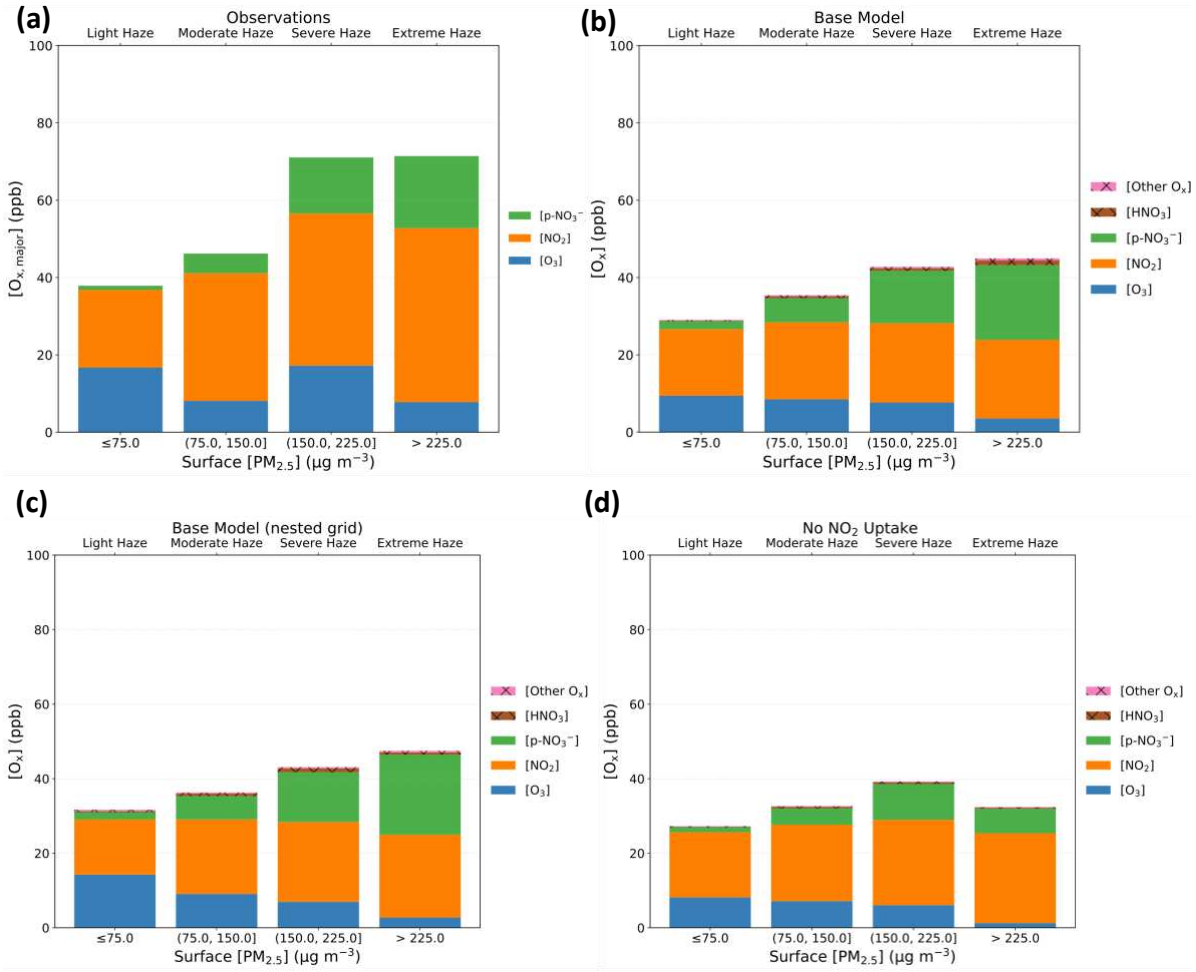

Figure 4. Concentration and speciation of O_x under different haze regimes in (a) observations, (b) base simulation, (c) nested-grid base simulation, (d) No NO_2 Uptake simulation. Hatching (x-filled bars) indicates the O_x species that were not measured at the observation sites.

425
426

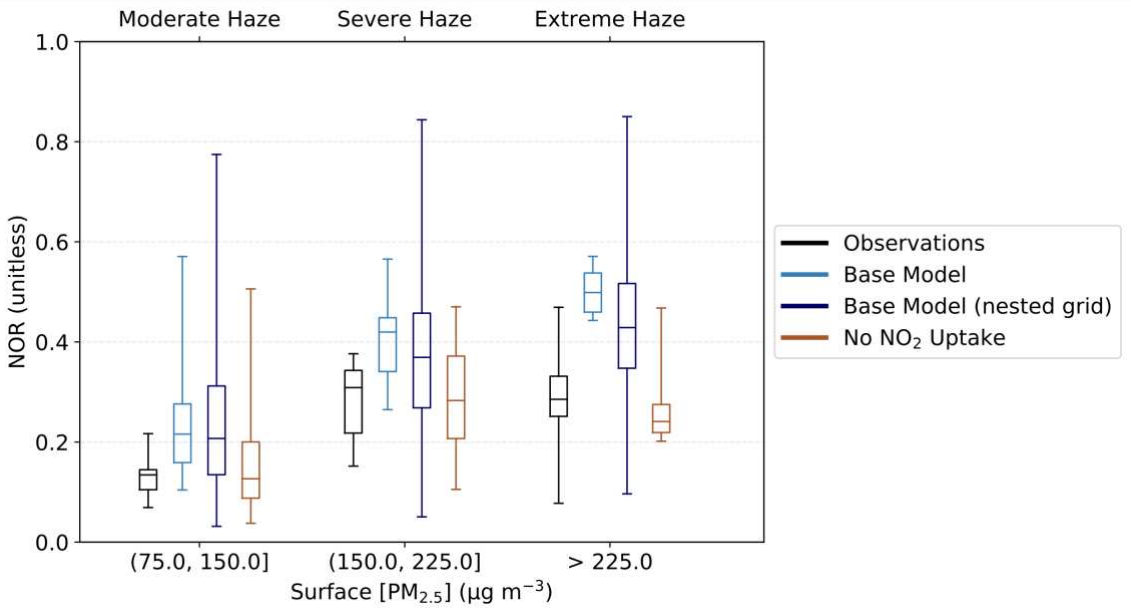

Figure 5. Comparison of nitrogen oxidation ratio (NOR) in observations and model simulations under different haze regimes.

427

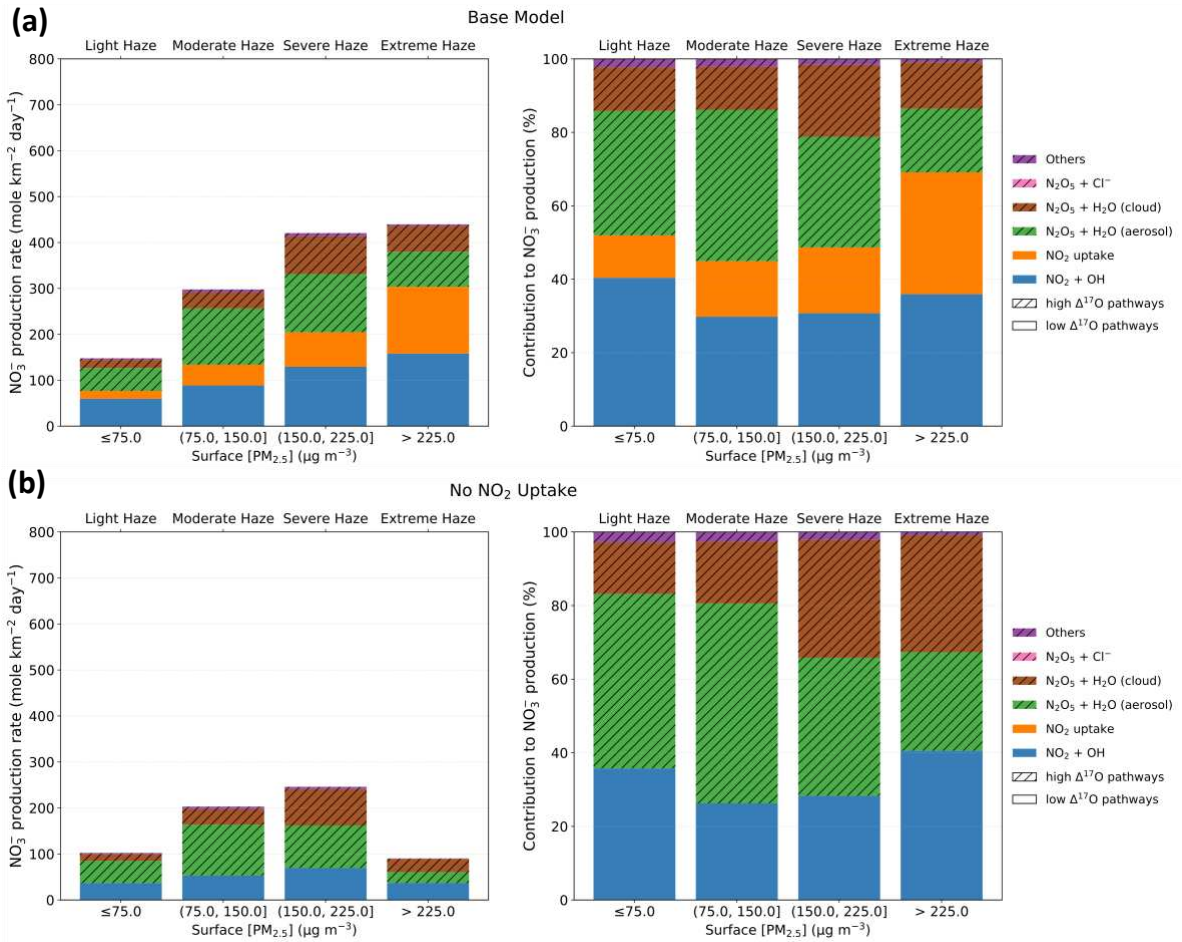

Figure 6. Average rate of different near-surface nitrate production pathways (left) and their relative contribution to nitrate formation in Beijing under different haze regimes (right) in (a) the base simulation and (b) No NO_2 Uptake simulation. "Near-surface" is defined as the sum over the ten lowest vertical levels in model, which on average corresponds to the altitudes between 0 to 1300 m. Hatching (//-filled bars) indicates high-$\Delta^{17}O$ pathways.

3.2.2 No-NO_2-uptake model simulation

An overestimate of NOR combined with the models' low bias in $\Delta^{17}O$ suggests an overestimate of NO_2 uptake (a low-$\Delta^{17}O$ heterogeneous pathway). Although a high bias in NOR could also suggest an underestimate of renoxification, a model sensitivity study allowing for efficient photolysis of p-NO_3^- shows that this explanation cannot resolve the model biases (Refer to Text S2.1 in SI). To evaluate the role of NO_2 uptake on the three chemistry metrics, we perform a sensitivity simulation in which the reaction is removed from the model by setting the uptake coefficients of NO_2 uptake on all types of aerosol and clouds to zero (i.e., $\gamma(NO_2) = 0$).

Without NO_2 uptake, the model predicts higher $\Delta^{17}O(NO_3^-)$ relative to the base model simulation under all haze regimes (Figure 3). The average increase in modeled $\Delta^{17}O(NO_3^-)$ in intense haze is 1.5 ‰, and the largest increase is found in extreme haze: the modeled median $\Delta^{17}O(NO_3^-)$ increases by 2.6 ‰ compared to the base simulation. Most of the modeled $\Delta^{17}O(NO_3^-)$ in

extreme haze now lie inside the range of observations. The simulation without NO_2 uptake predicts the median $\Delta^{17}O(NO_3^-)$ in extreme haze to be 29.9‰, which is closer to the observations (31.5‰). However, the model now overestimates the $\Delta^{17}O(NO_3^-)$ in moderate haze. The median $\Delta^{17}O(NO_3^-)$ in moderate haze in the model is 30.9‰, which is 2.0‰ higher than the observations. Similar to the base simulation, the simulation without NO_2 uptake predicts a decrease in $\Delta^{17}O(NO_3^-)$ as $[PM_{2.5}]$ increases. The negative relationship is driven by the sharp decrease in the rate of N_2O_5 production and nitrate production via N_2O_5 uptake in extreme haze (Figure 6).

The model without NO_2 uptake shows better agreement with observations of O_x speciation and NOR but still underestimates the total O_x concentration (Figure 4 and Figure 5). The average NOR in intense haze in the model is 0.22, which is very close to the observations (0.21). The modeled NOR in extreme haze spans within the observed range for all haze regimes (Figure 5). Modeled $[O_x]$ is not sensitive to the change in NO_2 uptake, except in extreme haze. $[O_x]$ in extreme haze decreases from 41.0 ppb in the base simulation to 34.6 ppb in the simulation with no NO_2 uptake. This worsens the underestimate of modeled $[O_x]$.

The reduction in NOR relative to the base model simulation is due to a reduction in the nitrate-production rate in all haze regimes, but especially during extreme haze (Figure 6). This is driven mainly by the absence of NO_2 uptake as a nitrate-production pathway, but also due to a decrease in nitrate production via NO_2 + OH. The decrease in nitrate production via NO_2 + OH is driven by the lack of HONO production from NO_2 uptake, the photolysis of which was a major source of OH in the model. The rate of N_2O_5 uptake remains relatively unchanged, except for a decrease during extreme haze (Figure 7). This increases the relative importance of N_2O_5 uptake resulting in an increase in $\Delta^{17}O(NO_3^-)$ during all haze regimes compared to the base model, especially during more intense haze events.

The results from the simulation without NO_2 uptake demonstrates that model discrepancies in $\Delta^{17}O(NO_3^-)$ and O_x as seen in the base simulation cannot be solely explained by the uncertainty in the efficiency of NO_2 uptake. Even when we completely eliminate the contribution of nitrate production from the NO_2 uptake pathway, the existing high-$\Delta^{17}O$ pathways in the model still cannot contribute enough to reproduce the observed range of $\Delta^{17}O(NO_3^-)$ in severe haze and extreme haze. This model sensitivity simulation also shows that the supply of $[NO_2]$ is not a rate-limiting factor for N_2O_5 uptake in Beijing. As less NO_2 is converted into NO_3^- due to the absence of NO_2 uptake pathway, the modeled $[O_3]$ becomes more depleted as $[NO_x]$ increases (Figure 4 and Figure S6). In the presence of excess NO_x, the low $[O_3]$ in the model slows down the production of NO_3 radicals via NO_2 + O_3, which ultimately limits the rate of N_2O_5 production via NO_2 + NO_3 and nitrate production via N_2O_5 uptake. Compared with the base simulation, the simulation without NO_2 uptake predicts lower N_2O_5 production and lower nitrate production via N_2O_5 uptake on aerosols and clouds in extreme haze (Figure 7), further supporting that O_3 is the limiting factor for N_2O_5 production and uptake.

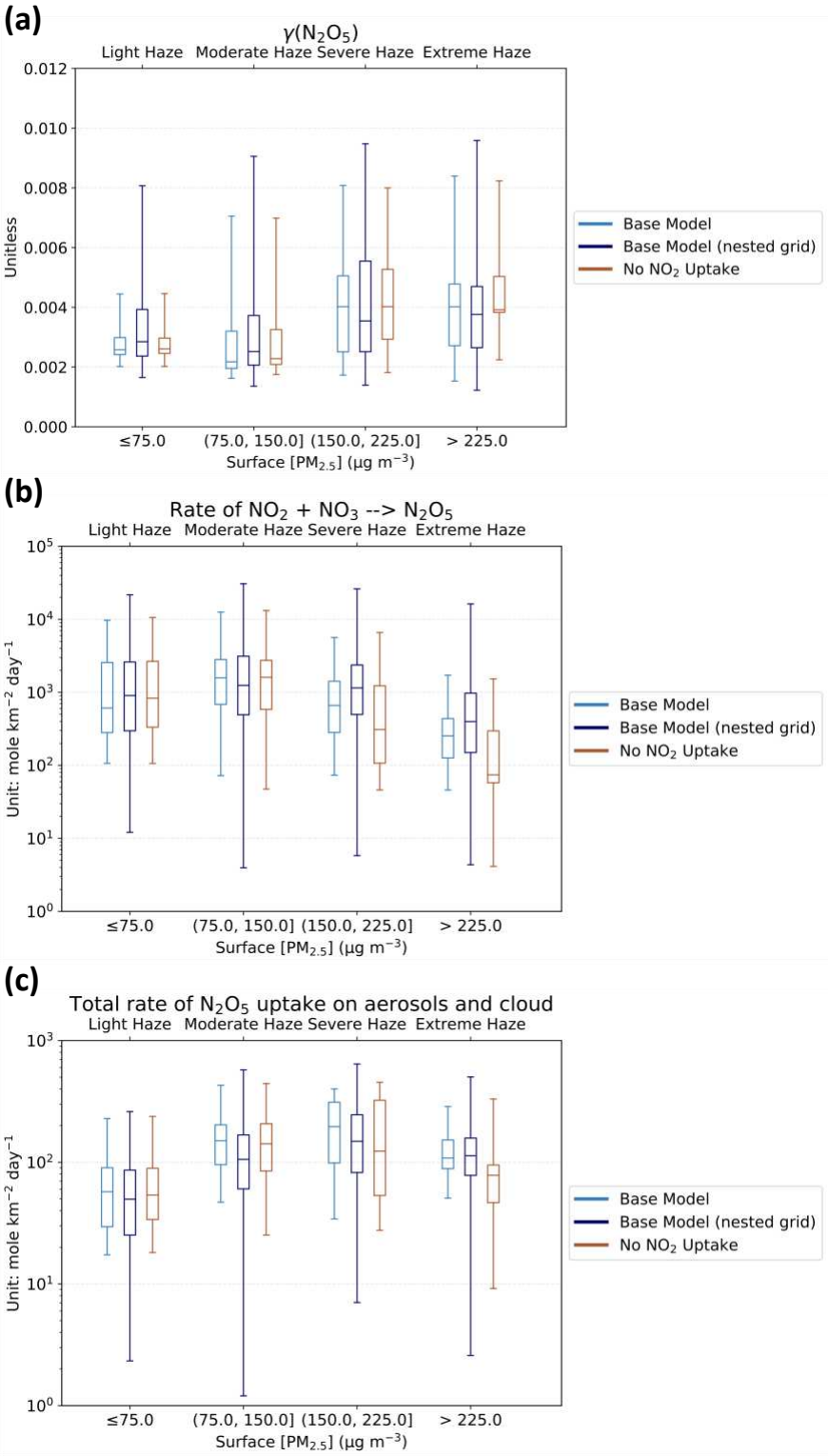

Figure 7. Factors controlling the near-surface rate of nitrate production via N_2O_5 hydrolysis in simulations and their dependence on [$PM_{2.5}$]. 7(a) shows the average uptake coefficient of N_2O_5 on aerosols. 7(b) shows the average rate of N_2O_5 production. 7(c) shows the average total rate of N_2O_5 uptake on aerosols and cloud.

487

4 Discussion

4.1 Model sensitivity to uncertainties in NO_2 uptake on aerosol

The model results presented in Section 3 and Text S2 show that modeled NOR and $\Delta^{17}O(NO_3^-)$ are most sensitive to NO_2 uptake. In NO_x-rich air, we expect to see positive relationships between $[HO_x]$ and $[O_3]$ because of their coupling via the cycling of NO_x (Bates & Jacob, 2020). As modeled O_3 concentration increases, NO more likely reacts with O_3 to produce NO_2, as a result, more HO_x becomes available for other reactions, including nitrate production, and vice versa. The competing effects of HO_x- and ozone-related nitrate-production pathways explain why modeled $\Delta^{17}O(NO_3^-)$ is not very sensitive to changes in various chemical parameters, with the exception of $\gamma(NO_2)$. NO_2 uptake, which carries a low-$\Delta^{17}O$ signature, is the only important nitrate-production pathway in the base model that converts NO_2 into NO_3^- without involving HO_x or ozone directly (Figure 1b). Additional model simulations increasing the HONO yield resulting from NO_2 uptake on aerosol to 100%, as well as model simulations including various combinations of the three model sensitivity studies described in Section 3.2 and Text S2, further show that $\Delta^{17}O(NO_3^-)$ and NOR are most sensitive to $\gamma(NO_2)$ (Figure S9 and Figure S10). The extra HONO produced from NO_2-uptake yielding 100% HONO increases OH and the rate of NO_2 + OH and simultaneously promotes nitrate production via N_2O_5 uptake through HO_x-O_3 coupling effects (See Figure S11), but the modeled $[O_x]$ is still low compared to the observations (Figure S12). Among all the model simulations performed, only those with $\gamma(NO_2) = 0$ improve model agreement with both observed $\Delta^{17}O(NO_3^-)$ and NOR during more intense haze events (Figure S9 and Figure S10).

In addition to the isotopic constraints, results from some laboratory and field studies also support the choice of a lower $\gamma(NO_2)$. The current GC parametrization sets $\gamma(NO_2$, black carbon$)=10^{-4}$, which is 20 times higher than $\gamma(NO_2$, SNA). Laboratory studies of NO_2(g) uptake on soot or carbonaceous surfaces suggested that heterogeneous reactions can rapidly consume the organic adsorbates and/or surface groups (Ammann et al., 1998; Bröske et al., 2003; Gerecke et al., 1998; Kalberer et al., 1999; Kleffmann et al., 1999), with rates of NO_2 uptake decreasing to negligible levels within minutes to hours (Gerecke et al., 1998; Kalberer et al., 1999; Kleffmann et al., 1999). For SNA aerosols, laboratory studies by F. Tan et al. (2016) and F. Tan et al. (2017) found that the rate of NO_2 uptake decreases with increasing RH when aerosols contain $CaCO_3$ due to formation of insoluble $CaSO_4 \cdot nH_2O$ on aerosol surfaces at higher RH. A potential suppressing effect of high-RH conditions on NO_2 uptake may help to explain the positive relationship between $\Delta^{17}O(NO_3^-)$ and $[PM_{2.5}]$ in observations. P. Liu et al. (2020) used the RH-dependence of NO_2 uptake to explain the negative relationship between NOR and RH when RH is above 60% in their Beijing observations. However, we cannot replicate their finding using our observations, which show a positive relationship between NOR and RH across all RH conditions (Figure S13). While some studies suggested that the heterogeneous reactions between NO_2 and SO_2 are important during wintertime haze events (e.g., Cheng et al., 2016; J. Wang et al., 2020), analysis of sulfate $\Delta^{17}O$ observations by Shao et al. (2019) showed that these reactions contribute less than 2% to heterogeneous formation of sulfate based on isotope observations in Beijing during the time period studied here. Given the large uncertainties of NO_2 uptake under atmospheric conditions and its large influence on nitrate production, HONO production, and $[O_x]$

in extreme haze, future studies should investigate the dominant mechanisms of NO_2 uptake on ambient aerosols and seek additional observational constraints during more intense haze events.

4.2 Possible causes of modeled underestimate in wintertime [O_x] in the North China Plain and their potential influence on NO_y chemistry

The model bias in wintertime ozone is critical for the simulation of [O_x] and nitrate production via N_2O_5 uptake. NO_2 and ozone are the major components of [O_x], but the base model underestimates their concentration in Beijing, especially during intense haze events. Modeled [NO_x] increases with [$PM_{2.5}$] in Beijing, and NO becomes the primary NO_x species in severe and extreme haze (Average [NO]/[NO_x] ratios are 0.55 and 0.66, respectively, in the base model. See Figure S6). The high [NO]/[NO_x] ratio on more polluted days is also evident in other wintertime observations in Beijing (Lu et al., 2019; Jiaqi Wang et al., 2017; G. Zhang et al., 2020). Under NO_x-saturated regime, the daytime cycling of NO and NO_2 is mainly controlled by the rates of NO + O_3 reaction (R3, a.k.a. ozone titration) and NO_2 photolysis. As predicted by the Leighton Relationship, [NO_2]/[NO] ratio is linearly proportional to [O_3] at photochemical steady state. From this basic theoretical perspective, the model bias in wintertime ozone should at least partly explain the underestimate in [NO_2] in our simulations. The actual NO_x-O_3 relationship may deviate from Leighton's prediction because of the complicated interaction between aerosols and radiation, which can affect the photolysis of NO_2 and O_3 (Hollaway et al., 2019; W. Wang et al., 2019). As explained in Section 3.2, low [O_3] can also limit nitrate production via N_2O_5 uptake in NO_x-rich air. Since ozone is a secondary pollutant that plays a central role in tropospheric chemistry, the formation of ozone is inevitably sensitive to many different chemical processes. The particulate-nitrate-photolysis and chlorine-chemistry simulations show improvement in reproducing [O_3] in intense haze in Beijing compared to the base simulation, but none of the proposed updates to NO_y and Cl_y chemistry investigated here can completely correct the model's overall bias in O_x in Beijing (See Figure S12 and Text S2). In this section, we discuss other chemical processes that may explain the modeled underestimate in wintertime [O_3] and [O_x].

4.2.1 Aerosol uptake of HO_2 radicals

The uptake of HO_2 radicals on aerosols has been suggested as a key process in driving the observed trends of ozone in China in the 2010s (J. Li et al., 2018; K. Li, Jacob, Liao, Shen, et al., 2019; K. Li, Jacob, Liao, Zhu, et al., 2019). Aerosols can scavenge gas-phase HO_2 radicals reducing [HO_x] and inhibiting ozone production. As pollution-control policies in China have reduced ambient [$PM_{2.5}$] in the 2010s, less HO_2 is scavenged by aerosols, resulting in increases in the ozone production efficiency. This theory on HO_x-O_3-aerosol interactions is consistent with the increasing trend of summertime ozone observed in China (K. Li, Jacob, Liao, Shen, et al., 2019; K. Li, Jacob, Liao, Zhu, et al., 2019).

Despite the potential impacts of aerosol uptake of HO_2 on ozone in urban air, the efficiency of this chemical process is still highly uncertain and may strongly depend on the content of aqueous transition-metal ions, the acidity, and the size of the aerosol (Guo et al., 2019; Mao et al., 2013; Thornton & Abbatt, 2005). To estimate the largest possible influence of HO_2 uptake on model

bias in [O_x] in intense haze, we consider the extreme case of $\gamma(HO_2) = 0$ on all aerosols (Denote as no HO_2 uptake simulation). Disabling the uptake of HO_2 on aerosols increases the modeled median [$O_{x,\,major}$] by 9.5% in intense haze, but this is smaller than the corresponding change resulting from introducing p-NO_3^- photolysis into the model (+24%) (See Figure S12 and Text S2). The model still fails to reproduce the high level of [O_x] in observations in intense haze. The overall effect of HO_2 uptake on NOR and $\Delta^{17}O(NO_3^-)$ are small in comparison with the models with $\gamma(NO_2) = 0$ (See Figure S9 and Figure S10). Our simulation results show that the uncertainty in $\gamma(HO_2)$ is not of primary importance to the model bias in simulating [O_x], NOR, and $\Delta^{17}O(NO_3^-)$ in Beijing.

4.2.2 Wintertime emissions of volatile organic compounds in the North China Plain

The roles of VOCs in nitrate production have been highlighted in recent studies of nitrate pollution in urban air (Fu et al., 2020; He et al., 2018; Shah et al., 2020; W. Song et al., 2020; Y. Wang et al., 2019; Womack et al., 2019). In Text S1, we showed that the direct effects of VOCs on nitrate formation are likely small in wintertime Beijing. However, VOCs can still modulate nitrate production rates by influencing ozone formation (Huang et al., 2021; Womack et al., 2019). VOCs accelerate the production of O_3 in NO_x-rich urban air. Reduction in VOC emissions has been proposed as a key strategy for mitigating wintertime nitrate pollution in Beijing and in Utah (Lu et al., 2019; Womack et al., 2019). Because of the potential importance of [VOCs] in nitrate production during intense haze events, we investigate the model bias in simulating wintertime [VOCs] in Beijing and examine whether a bias in [VOCs] can explain the model-observation discrepancy in terms of [O_x].

Emitted from biomass burning and fossil fuels, aromatic compounds are often considered to be the largest contributor to ozone formation in metropolitan areas in China (J. Sun et al., 2018; Yan et al., 2017; D. Yu et al., 2020). The concentration of aromatics in general positively correlates with [$PM_{2.5}$] in the model (Table S3), consistent with observations in the North China Plain (C. Liu et al., 2017; Sheng et al., 2018; J. Sun et al., 2018). However, the model underestimates the concentration of aromatics compared to the observations, except for xylene. The mean concentration of benzene in the base simulation is lower than the wintertime observations in Beijing by a factor of 2 (see Table S3). Le et al. (2020) showed that a 30% increase in the emissions of VOCs from conventional anthropogenic sources can increase the wintertime [O_3] by about 10% in their model. Model bias in wintertime VOC emissions from industry and transportation could be an important reason for the underestimate of modeled [O_x] during intense haze events.

Recent studies suggested that the manufacture and consumption of volatile chemical products (VCPs) can be an overlooked anthropogenic VOC-emission source in air-quality models (e.g., McDonald et al., 2018). Throughout the product life cycle, these VCPs emit many complex VOCs, including C≥4 alkanes, alcohols, and terpenes, and may account for about half of the VOC reactivity with OH in Los Angeles (McDonald et al., 2018). Comparison of the concentration of these VCP-related VOCs in the base simulation with wintertime observations in Beijing shows a model underestimate of the concentration of alcohols, monoterpenes, and C≥4 alkanes in Beijing (See Table S3). However, without more observational constraints on the fluxes

and speciation of VCP emissions in the North China Plain and their dependencies on atmospheric conditions, it is hard to conclude whether the model bias in [O_x] can be reduced by including emissions of VCPs in the simulations.

4.3 Examination of the non-linearity in nitrate chemistry

The weak response of particulate nitrate and other secondary aerosols to the reduction in NO_x emissions has been noted in studies of the long-term trends in wintertime air quality (e.g., H. Li et al., 2019; Shah et al., 2018; Xu et al., 2019), and more recently, in studies of air quality during the COVID-19 pandemic (Diamond & Wood, 2020; Huang et al., 2021; Le et al., 2020; Y. Sun et al., 2020). An astonishing example of the complexity of this NO_x-aerosol relationship can be found in the observations in the North China Plain from January to March in year 2020. Following a 40-60% reduction in the NO_x emissions over the North China Plain caused by COVID-19 lockdown, observed [$PM_{2.5}$], paradoxically, increased by 50% or more at several stations near Beijing (Huang et al., 2021; Le et al., 2020). Studies suggested that the surge is mostly driven by the production of secondary aerosols, including p-NO_3^- (Huang et al., 2021; Le et al., 2020).

Many studies attributed the persistence of high levels of p-NO_3^- to the non-linearity in atmospheric chemistry, but they hypothesized different mechanisms. Shah et al. (2018) suggested that NO_x and SO_2 emission reductions over the eastern United States has resulted in a gradual increase in aerosol alkalinity, which favors HNO_3-to-p-NO_3^- conversion and increases the fraction of p-NO_3^- in wintertime aerosols. We denote the non-linearity originated from the sensitivity of p-NO_3^- to aerosol-pH as the 'alkalinity-limited mechanism'. In contrast, studies in China observed an increase in [O_3] and production of secondary aerosols following the emission reductions during COVID-19 lockdown, which is likely caused by a reduction in ozone titration (Huang et al., 2021; Le et al., 2020). The enhancement in [O_3] increases the oxidizing capacity of the lower troposphere and promotes the production of secondary aerosols (Fu et al., 2020; Huang et al., 2021; Le et al., 2020). We denote the non-linearity arising from the sensitivity of nitrate to NO_x-VOCs-ozone chemistry as the 'ozone-limited mechanism'.

To examine the relevance of ozone-limited mechanism in our model simulations of nitrate production, we analyze the relationship between nitrate production rate, [O_3], and [NO_x] during intense haze events for Beijing (Figure 8). It is noted that the inter-model differences in our study orginates from the variations in the modeled chemistry. This is different from other studies like Huang et al. (2021), where they focused on the effects of changing emissions. Although the modeled [O_3], [NO_x], and nitrate production rate are considerably different among various experiments, a positive relationship between nitrate production rate and [O_3] during intense haze events can be identified in all the simulations with $\gamma(NO_2) = 0$. In contrast, all these simulations predict a negative relationship between the nitrate production rate and [NO_x], which can be attributed to the effects of ozone titration. The strong and postive correlation between the nitrate production rate and [O_3] predicted by our models is consistent with the theory of ozone-limited mechanism. Meanwhile, our simulations also show that the partitioning between p-NO_3^- and HNO_3 in Beijing is not sensitive to the intensity of haze events or the difference in NO_y chemistry parametrization (See Figure S14). p-NO_3^- remains the dominant form of NO_3^- in all

cases. The model prediction is also consistent with the estimated high aerosol pH (4.5 ± 0.7) in wintertime Beijing, which can be explained by the high NH_3 abundance in observations (Ding et al., 2019). Our model simulations confirm the importance of ozone-limited mechanism in wintertime North China Plain and show that the positive relationship between [O_3] and nitrate production rate during intense haze events is robust regardless of the uncertainty in modeled NO_y chemistry after $\gamma(NO_2)$ is set to 0.

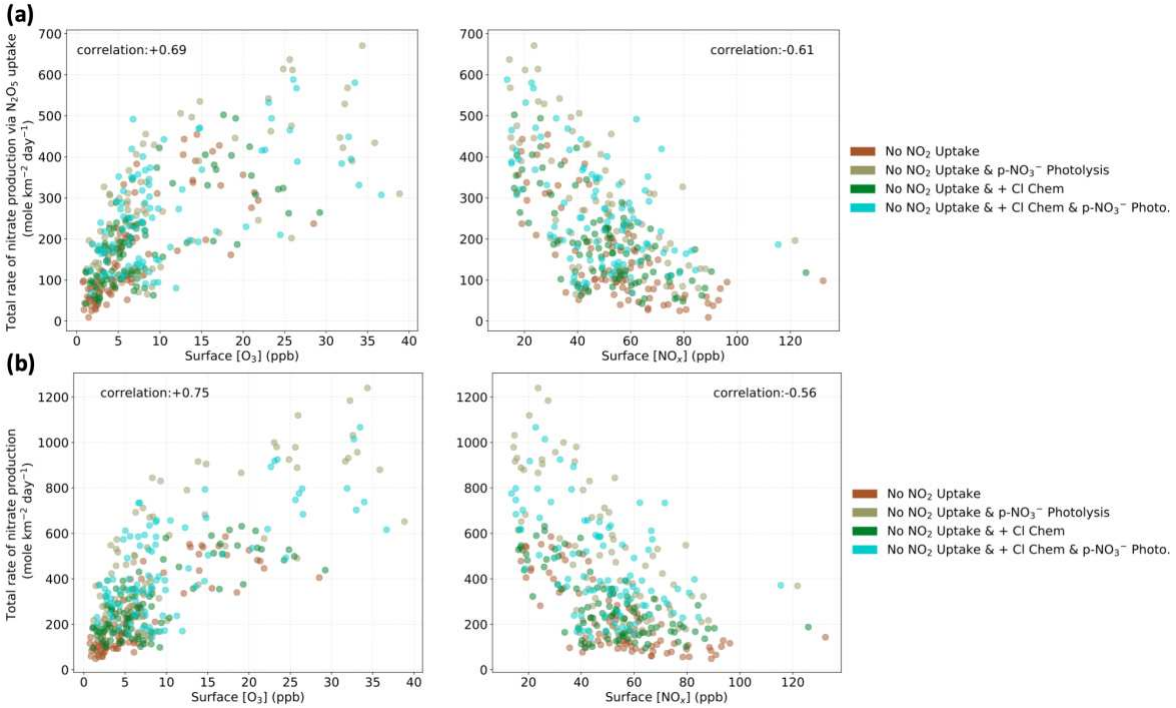

Figure 8. The relationship between [O_3], [NO_x], the rate of nitrate production via N_2O_5 uptake (8a), and the total rate of nitrate production (8b) during intense haze events in simulations without NO_2 uptake on aerosols. The correlation coefficients shown in the figure are calculated using data from all the four model experiments. All the estimated linear-regression slopes are different from 0 at the 95% significance level.

5 Conclusions and Implications

By analyzing the observations of $\Delta^{17}O(NO_3^-)$, NOR, and O_x in Beijing during winter 2014-15 and results from a global and regional chemical transport model, we examine the mechanisms for nitrate production in wintertime North China Plain and how the underlying chemical processes vary with the intensity of haze events. $\Delta^{17}O(NO_3^-)$ indicates the dominance of high-$\Delta^{17}O$ oxidants (e.g., ozone) to low-$\Delta^{17}O$ oxidants (e.g., OH and RO_2) during NO_x-to-NO_3^- conversion, while NOR and O_x provide information about the efficiency of NO_y oxidation and the oxidizing capacity of the air. In intense haze, the base model underestimates $\Delta^{17}O(NO_3^-)$ and [O_x] in Beijing by – 0.86 ‰ and − 36%, respectively, but overestimates NOR by +0.12. To investigate the relationship between model bias and uncertainty in chemistry, we perform model sensitivity experiments by varying several key parameters in NO_y chemistry. Our analysis suggests a model

overestimate in NO_2-uptake rate on aerosols and the underestimate in wintertime ozone may explain the model biases.

Our model sensitivity simulations show that modeled $\Delta^{17}O(NO_3^-)$ and NOR during highly polluted conditions are most sensitive to the parametrization of NO_2 uptake on aerosols. The $\Delta^{17}O(NO_3^-)$ observations in Beijing and its relationship with $[PM_{2.5}]$ suggest that the rate of NO_2 uptake is likely too high in the model, yielding too high nitrate- and HONO-production rates in more intense haze. Model simulations without NO_2 uptake better reproduce the observed $\Delta^{17}O(NO_3^-)$ and NOR in Beijing under high-$PM_{2.5}$ conditions. A NO_2 uptake mechanism that is suppressed by high RH may explain the positive relationship between $\Delta^{17}O(NO_3^-)$ and $[PM_{2.5}]$ in observations, but the supporting evidence for such a mechanism is currently inconclusive. Further laboratory and field studies are needed to constrain the reaction probability of NO_2 on ambient aerosols, with a focus on its role in nitrate and HONO formation.

Our simulations also reveal that nitrate production is largely limited by ozone during intense haze events in wintertime North China Plain. After accounting for the uncertainty in NO_2 uptake on aerosols, our analysis suggests that N_2O_5 uptake in aerosols and clouds is the dominant mechanism for nitrate production in wintertime Beijing. Under high-NO_x-high-$PM_{2.5}$ conditions, $[O_3]$ modulates N_2O_5 production and, subsequently, the rate of nitrate production via N_2O_5 uptake. The base model underestimates $[O_3]$ and $[O_x]$ during wintertime haze events. Uncertainty in heterogeneous chemical processes, such as renoxification via nitrate photolysis or $ClNO_2$ production and the scavenging of HO_x by aerosols, may contribute to the model bias in wintertime O_x, but our simulations show that adjusting related chemistry parameters cannot remove the bias even under extreme scenarios, suggesting processes other than chemistry (e.g., emissions of VCPs and feedbacks involving aerosol-boundary-layer interaction) may play a more important role. Both the reduction in $[PM_{2.5}]$ and NO_x emissions have been shown to lead to increases in $[O_3]$ in the North China Plain (Huang et al., 2021; Le et al., 2020; K. Li, Jacob, Liao, Zhu, et al., 2019). Nitrate production rates may continue to increase as long as $[O_3]$ increases despite decreases in $[NO_x]$, creating a negative feedback that reduces the effectiveness of air pollution reduction strategies. Policies that result in a reduction of ambient O_3 concentrations, possibly through reductions in VOC emissions, will also reduce the formation of nitrate and its contribution to $PM_{2.5}$ during wintertime haze events.

Acknowledgments and Data

This work was supported by funding from the National Science Foundation (NSF) to B.A. (Grant AGS 1644998). Y.C.C. acknowledges helpful discussions with Brian Boys from Dalhousie University, Men Xia from the Hong Kong Polytechnic University, and Wei Zhou from the Chinese Academy of Sciences. P.Z.H acknowledges the funding support from the Natural Science Foundation of AnHui Province, China (Grant 2008085QD184). C.D.H acknowledges the funding support from National Aeronautics and Space Administration (NASA) (Grant NNX16AI57G). L.J. acknowledges the funding support from NSF (Grant AGS-1901786). J.A.T. acknowledges the funding support from NSF (Grant AGS-1652688). Z.Q.X. acknowledges the funding support from the National Key Project of Ministry of Science and Technology of the People's Republic of China (Grant 2016YFC0203302). Data used in this study is hosted in the

737 University of Washington's ResearchWorks Archive and can be accessed online
738 (http://hdl.handle.net/1773/46927).
739

References

Alexander, B., Sherwen, T., Holmes, C. D., Fisher, J. A., Chen, Q., Evans, M. J., & Kasibhatla, P. (2020). Global inorganic nitrate production mechanisms: comparison of a global model with nitrate isotope observations. *Atmospheric Chemistry and Physics*, *20*(6), 3859–3877. https://doi.org/10.5194/acp-20-3859-2020

Ammann, M., Kalberer, M., Jost, D. T., Tobler, L., Rössler, E., Piguet, D., et al. (1998). Heterogeneous production of nitrous acid on soot in polluted air masses. *Nature*, *395*(6698), 157–160. https://doi.org/10.1038/25965

An, Z., Huang, R.-J., Zhang, R., Tie, X., Li, G., Cao, J., et al. (2019). Severe haze in northern China: A synergy of anthropogenic emissions and atmospheric processes. *Proceedings of the National Academy of Sciences of the United States of America*, *116*(18), 8657–8666. https://doi.org/10.1073/pnas.1900125116

Bao, F., Li, M., Zhang, Y., Chen, C., & Zhao, J. (2018). Photochemical Aging of Beijing Urban PM $_{2.5}$: HONO Production. *Environmental Science & Technology*, *52*(11), 6309–6316. https://doi.org/10.1021/acs.est.8b00538

Bates, K. H., & Jacob, D. J. (2020). An Expanded Definition of the Odd Oxygen Family for Tropospheric Ozone Budgets: Implications for Ozone Lifetime and Stratospheric Influence. *Geophysical Research Letters*, *47*(4). https://doi.org/10.1029/2019GL084486

Bertram, T. H., & Thornton, J. A. (2009). Toward a general parameterization of N2O5 reactivity on aqueous particles: The competing effects of particle liquid water, nitrate and chloride. *Atmospheric Chemistry and Physics*, *9*(21), 8351–8363. https://doi.org/10.5194/acp-9-8351-2009

Bröske, R., Kleffmann, J., & Wiesen, P. (2003). Heterogeneous conversion of NO2 on secondary organic aerosol surfaces: A possible source of nitrous acid (HONO) in the atmosphere? *Atmospheric Chemistry and Physics*, *3*(3), 469–474. https://doi.org/10.5194/acp-3-469-2003

Chen, S., Wang, H., Lu, K., Zeng, L., Hu, M., & Zhang, Y. (2020). The trend of surface ozone in Beijing from 2013 to 2019: Indications of the persisting strong atmospheric oxidation capacity. *Atmospheric Environment*, *242*, 117801. https://doi.org/10.1016/j.atmosenv.2020.117801

Chen, Y., Ebenstein, A., Greenstone, M., & Li, H. (2013). Evidence on the impact of sustained exposure to air pollution on life expectancy from China's Huai River policy. *Proceedings of the National Academy of Sciences of the United States of America*, *110*(32), 12936–12941. https://doi.org/10.1073/pnas.1300018110

Cheng, Y., Zheng, G., Wei, C., Mu, Q., Zheng, B., Wang, Z., et al. (2016). Reactive nitrogen chemistry in aerosol water as a source of sulfate during haze events in China. *Science Advances*, *2*(12), e1601530. https://doi.org/10.1126/sciadv.1601530

Diamond, M. S., & Wood, R. (2020). Limited Regional Aerosol and Cloud Microphysical Changes Despite Unprecedented Decline in Nitrogen Oxide Pollution During the February 2020 COVID-19 Shutdown in China. *Geophysical Research Letters*, *47*(17). https://doi.org/10.1029/2020GL088913

Ding, J., Zhao, P., Su, J., Dong, Q., Du, X., & Zhang, Y. (2019). Aerosol pH and its driving

781 factors in Beijing. *Atmospheric Chemistry and Physics*, *19*(12), 7939–7954.
782 https://doi.org/10.5194/acp-19-7939-2019

783 Eastham, S. D., Weisenstein, D. K., & Barrett, S. R. H. (2014). Development and evaluation of
784 the unified tropospheric–stratospheric chemistry extension (UCX) for the global chemistry-
785 transport model GEOS-Chem. *Atmospheric Environment*, *89*, 52–63.
786 https://doi.org/10.1016/j.atmosenv.2014.02.001

787 Fisher, J. A., Atlas, E. L., Barletta, B., Meinardi, S., Blake, D. R., Thompson, C. R., et al. (2018).
788 Methyl, Ethyl, and Propyl Nitrates: Global Distribution and Impacts on Reactive Nitrogen
789 in Remote Marine Environments. *Journal of Geophysical Research: Atmospheres*, *123*(21),
790 12,429-12,451. https://doi.org/10.1029/2018JD029046

791 Fountoukis, C., & Nenes, A. (2007). *Atmospheric Chemistry and Physics ISORROPIA II: a*
792 *computationally efficient thermodynamic equilibrium model for K +-Ca 2+-Mg 2+-NH +*
793 *4-Na +-SO 2− 4-NO − 3-Cl −-H 2 O aerosols*. *Atmos. Chem. Phys* (Vol. 7). Retrieved from
794 www.atmos-chem-phys.net/7/4639/2007/

795 Fu, X., Wang, T., Gao, J., Wang, P., Liu, Y., Wang, S., et al. (2020). Persistent Heavy Winter
796 Nitrate Pollution Driven by Increased Photochemical Oxidants in Northern China.
797 *Environmental Science and Technology*, *54*(7), 3881–3889.
798 https://doi.org/10.1021/acs.est.9b07248

799 Gaston, C. J., Thornton, J. A., & Ng, N. L. (2014). Reactive uptake of N_2O_5 to internally mixed
800 inorganic and organic particles: the role of organic carbon oxidation state and inferred
801 organic phase separations. *Atmospheric Chemistry and Physics*, *14*(11), 5693–5707.
802 https://doi.org/10.5194/acp-14-5693-2014

803 Geng, L., Murray, L. T., Mickley, L. J., Lin, P., Fu, Q., Schauer, A. J., & Alexander, B. (2017).
804 Isotopic evidence of multiple controls on atmospheric oxidants over climate transitions.
805 *Nature*, *546*(7656), 133–136. https://doi.org/10.1038/nature22340

806 Gerecke, A., Thielmann, A., Gutzwiller, L., & Rossi, M. J. (1998). The chemical kinetics of
807 HONO formation resulting from heterogeneous interaction of NO 2 with flame soot.
808 *Geophysical Research Letters*, *25*(13), 2453–2456. https://doi.org/10.1029/98GL01796

809 Guo, J., Wang, Z., Tao Wang, & Zhang, X. (2019). Theoretical evaluation of different factors
810 affecting the HO2 uptake coefficient driven by aqueous-phase first-order loss reaction.
811 *Science of The Total Environment*, *683*, 146–153.
812 https://doi.org/10.1016/j.scitotenv.2019.05.237

813 He, P., Xie, Z., Chi, X., Yu, X., Fan, S., Kang, H., et al. (2018). Atmospheric Δ 17 O(NO 3 −)
814 reveals nocturnal chemistry dominates nitrate production in Beijing haze. *Atmospheric*
815 *Chemistry and Physics*, *18*(19), 14465–14476. https://doi.org/10.5194/acp-18-14465-2018

816 Hoesly, R. M., Smith, S. J., Feng, L., Klimont, Z., Janssens-Maenhout, G., Pitkanen, T., et al.
817 (2018). Historical (1750–2014) anthropogenic emissions of reactive gases and aerosols
818 from the Community Emissions Data System (CEDS). *Geoscientific Model Development*,
819 *11*(1), 369–408. https://doi.org/10.5194/gmd-11-369-2018

820 Hollaway, M., Wild, O., Yang, T., Sun, Y., Xu, W., Xie, C., et al. (2019). Photochemical impacts
821 of haze pollution in an urban environment. *Atmospheric Chemistry and Physics*, *19*(15),
822 9699–9714. https://doi.org/10.5194/acp-19-9699-2019

Holmes, C. D., Bertram, T. H., Confer, K. L., Graham, K. A., Ronan, A. C., Wirks, C. K., & Shah, V. (2019). The Role of Clouds in the Tropospheric NOx Cycle: A New Modeling Approach for Cloud Chemistry and Its Global Implications. *Geophysical Research Letters*, *46*(9), 4980–4990. https://doi.org/10.1029/2019GL081990

Huang, X., Ding, A., Wang, Z., Ding, K., Gao, J., Chai, F., & Fu, C. (2020). Amplified transboundary transport of haze by aerosol–boundary layer interaction in China. *Nature Geoscience*, *13*(6), 428–434. https://doi.org/10.1038/s41561-020-0583-4

Huang, X., Ding, A., Gao, J., Zheng, B., Zhou, D., Qi, X., et al. (2021). Enhanced secondary pollution offset reduction of primary emissions during COVID-19 lockdown in China. *National Science Review*, *8*(2). https://doi.org/10.1093/nsr/nwaa137

Hudman, R. C., Moore, N. E., Mebust, A. K., Martin, R. V, Russell, A. R., Valin, L. C., & Cohen, R. C. (2012). Steps towards a mechanistic model of global soil nitric oxide emissions: implementation and space based-constraints. *Atmospheric Chemistry and Physics*, *12*(16), 7779–7795. https://doi.org/10.5194/acp-12-7779-2012

Itahashi, S., Yumimoto, K., Uno, I., Hayami, H., Fujita, S., Pan, Y., & Wang, Y. (2018). A 15-year record (2001–2015) of the ratio of nitrate to non-sea-salt sulfate in precipitation over East Asia. *Atmospheric Chemistry and Physics*, *18*(4), 2835–2852. https://doi.org/10.5194/acp-18-2835-2018

Jaeglé, L., Shah, V., Thornton, J. A., Lopez-Hilfiker, F. D., Lee, B. H., McDuffie, E. E., et al. (2018). Nitrogen Oxides Emissions, Chemistry, Deposition, and Export Over the Northeast United States During the WINTER Aircraft Campaign. *Journal of Geophysical Research: Atmospheres*, *123*(21), 12,368-12,393. https://doi.org/10.1029/2018JD029133

Kalberer, M., Ammann, M., Arens, F., Gäggeler, H. W., & Baltensperger, U. (1999). Heterogeneous formation of nitrous acid (HONO) on soot aerosol particles. *Journal of Geophysical Research: Atmospheres*, *104*(D11), 13825–13832. https://doi.org/10.1029/1999JD900141

Kasibhatla, P., Sherwen, T., Evans, M. J., Carpenter, L. J., Reed, C., Alexander, B., et al. (2018). Global impact of nitrate photolysis in sea-salt aerosol on NOx, OH, and O3 in the marine boundary layer. *Atmospheric Chemistry and Physics*, *18*(15), 11185–11203. https://doi.org/10.5194/acp-18-11185-2018

Kenagy, H. S., Sparks, T. L., Ebben, C. J., Wooldrige, P. J., Lopez-Hilfiker, F. D., Lee, B. H., et al. (2018). NO x Lifetime and NO y Partitioning During WINTER. *Journal of Geophysical Research: Atmospheres*, *123*(17), 9813–9827. https://doi.org/10.1029/2018JD028736

Kleffmann, J., Becker, K. H., Lackhoff, M., & Wiesen, P. (1999). Heterogeneous conversion of NO2 on carbonaceous surfaces. *Physical Chemistry Chemical Physics*, *1*(24), 5443–5450. https://doi.org/10.1039/a905545b

Lamsal, L. N., Martin, R. V., van Donkelaar, A., Steinbacher, M., Celarier, E. A., Bucsela, E., et al. (2008). Ground-level nitrogen dioxide concentrations inferred from the satellite-borne Ozone Monitoring Instrument. *Journal of Geophysical Research*, *113*(D16), D16308. https://doi.org/10.1029/2007JD009235

Le, T., Wang, Y., Liu, L., Yang, J., Yung, Y. L., Li, G., & Seinfeld, J. H. (2020). Unexpected air pollution with marked emission reductions during the COVID-19 outbreak in China.

Science, *369*(6504), 702–706. https://doi.org/10.1126/science.abb7431

Lelieveld, J., Evans, J. S., Fnais, M., Giannadaki, D., & Pozzer, A. (2015). The contribution of outdoor air pollution sources to premature mortality on a global scale. *Nature*, *525*(7569), 367–371. https://doi.org/10.1038/nature15371

Leung, D. M., Shi, H., Zhao, B., Wang, J., Ding, E. M., Gu, Y., et al. (2020). Wintertime Particulate Matter Decrease Buffered by Unfavorable Chemical Processes Despite Emissions Reductions in China. *Geophysical Research Letters*, *47*(14). https://doi.org/10.1029/2020GL087721

Li, H., Cheng, J., Zhang, Q., Zheng, B., Zhang, Y., Zheng, G., & He, K. (2019). Rapid transition in winter aerosol composition in Beijing from 2014 to 2017: response to clean air actions. *Atmospheric Chemistry and Physics*, *19*(17), 11485–11499. https://doi.org/10.5194/acp-19-11485-2019

Li, J., Chen, X., Wang, Z., Du, H., Yang, W., Sun, Y., et al. (2018). Radiative and heterogeneous chemical effects of aerosols on ozone and inorganic aerosols over East Asia. *Science of the Total Environment*, *622–623*, 1327–1342. https://doi.org/10.1016/j.scitotenv.2017.12.041

Li, K., Jacob, D. J., Liao, H., Zhu, J., Shah, V., Shen, L., et al. (2019). A two-pollutant strategy for improving ozone and particulate air quality in China. *Nature Geoscience*, *12*(11), 906–910. https://doi.org/10.1038/s41561-019-0464-x

Li, K., Jacob, D. J., Liao, H., Shen, L., Zhang, Q., & Bates, K. H. (2019). Anthropogenic drivers of 2013-2017 trends in summer surface ozone in China. *Proceedings of the National Academy of Sciences of the United States of America*, *116*(2), 422–427. https://doi.org/10.1073/pnas.1812168116

Li, L., Hoffmann, M. R., & Colussi, A. J. (2018). Role of Nitrogen Dioxide in the Production of Sulfate during Chinese Haze-Aerosol Episodes. *Environmental Science & Technology*, *52*(5), 2686–2693. https://doi.org/10.1021/acs.est.7b05222

Li, M., Zhang, Q., Kurokawa, J., Woo, J.-H., He, K., Lu, Z., et al. (2017). MIX: a mosaic Asian anthropogenic emission inventory under the international collaboration framework of the MICS-Asia and HTAP. *Atmospheric Chemistry and Physics*, *17*(2), 935–963. https://doi.org/10.5194/acp-17-935-2017

Lin, J. T., & McElroy, M. B. (2010). Impacts of boundary layer mixing on pollutant vertical profiles in the lower troposphere: Implications to satellite remote sensing. *Atmospheric Environment*, *44*(14), 1726–1739. https://doi.org/10.1016/j.atmosenv.2010.02.009

Liu, C., Ma, Z., Mu, Y., Liu, J., Zhang, C., Zhang, Y., et al. (2017). The levels, variation characteristics, and sources of atmospheric non-methane hydrocarbon compounds during wintertime in Beijing, China. *Atmospheric Chemistry and Physics*, *17*(17), 10633–10649. https://doi.org/10.5194/acp-17-10633-2017

Liu, H., Jacob, D. J., Bey, I., & Yantosca, R. M. (2001). Constraints from 210 Pb and 7 Be on wet deposition and transport in a global three-dimensional chemical tracer model driven by assimilated meteorological fields. *Journal of Geophysical Research: Atmospheres*, *106*(D11), 12109–12128. https://doi.org/10.1029/2000JD900839

Liu, P., Ye, C., Xue, C., Zhang, C., Mu, Y., & Sun, X. (2020). Formation mechanisms of

atmospheric nitrate and sulfate during the winter haze pollution periods in Beijing: gas-phase, heterogeneous and aqueous-phase chemistry. *Atmospheric Chemistry and Physics*, *20*(7), 4153–4165. https://doi.org/10.5194/acp-20-4153-2020

Liu, Y., Lu, K., Li, X., Dong, H., Tan, Z., Wang, H., et al. (2019). A Comprehensive Model Test of the HONO Sources Constrained to Field Measurements at Rural North China Plain. *Environmental Science & Technology*, *53*(7), 3517–3525. https://doi.org/10.1021/acs.est.8b06367

Lu, K., Fuchs, H., Hofzumahaus, A., Tan, Z., Wang, H., Zhang, L., et al. (2019). Fast Photochemistry in Wintertime Haze: Consequences for Pollution Mitigation Strategies. *Environmental Science & Technology*, *53*(18), 10676–10684. https://doi.org/10.1021/acs.est.9b02422

Mao, J., Fan, S., Jacob, D. J., & Travis, K. R. (2013). Radical loss in the atmosphere from Cu-Fe redox coupling in aerosols. *Atmospheric Chemistry and Physics*, *13*(2), 509–519. https://doi.org/10.5194/acp-13-509-2013

Marais, E. A., & Wiedinmyer, C. (2016). Air Quality Impact of Diffuse and Inefficient Combustion Emissions in Africa (DICE-Africa). *Environmental Science & Technology*, *50*(19), 10739–10745. https://doi.org/10.1021/acs.est.6b02602

McDonald, B. C., De Gouw, J. A., Gilman, J. B., Jathar, S. H., Akherati, A., Cappa, C. D., et al. (2018). Volatile chemical products emerging as largest petrochemical source of urban organic emissions. *Science*, *359*(6377), 760–764. https://doi.org/10.1126/science.aaq0524

McDuffie, E. E., Fibiger, D. L., Dubé, W. P., Lopez-Hilfiker, F., Lee, B. H., Thornton, J. A., et al. (2018). Heterogeneous N2O5 Uptake During Winter: Aircraft Measurements During the 2015 WINTER Campaign and Critical Evaluation of Current Parameterizations. *Journal of Geophysical Research: Atmospheres*, *123*(8), 4345–4372. https://doi.org/10.1002/2018JD028336

Michalski, G., Scott, Z., Kabiling, M., & Thiemens, M. H. (2003). First measurements and modeling of Δ 17 O in atmospheric nitrate. *Geophysical Research Letters*, *30*(16). https://doi.org/10.1029/2003GL017015

Morin, S., Sander, R., & Savarino, J. (2011). Simulation of the diurnal variations of the oxygen isotope anomaly (Δ17O) of reactive atmospheric species. *Atmospheric Chemistry and Physics*, *11*(8), 3653–3671. https://doi.org/10.5194/acp-11-3653-2011

Murray, L. T., Jacob, D. J., Logan, J. A., Hudman, R. C., & Koshak, W. J. (2012). Optimized regional and interannual variability of lightning in a global chemical transport model constrained by LIS/OTD satellite data. *Journal of Geophysical Research: Atmospheres*, *117*(D20). https://doi.org/10.1029/2012JD017934

Neu, J. L., Prather, M. J., & Penner, J. E. (2007). Global atmospheric chemistry: Integrating over fractional cloud cover. *Journal of Geophysical Research*, *112*(D11), D11306. https://doi.org/10.1029/2006JD008007

Reed, C., Evans, M. J., Di Carlo, P., Lee, J. D., & Carpenter, L. J. (2016). Interferences in photolytic NO₂ measurements: explanation for an apparent missing oxidant? *Atmospheric Chemistry and Physics*, *16*(7), 4707–4724. https://doi.org/10.5194/acp-16-4707-2016

948 Savarino, J., Morin, S., Erbland, J., Grannec, F., Patey, M. D., Vicars, W., et al. (2013). Isotopic
949 composition of atmospheric nitrate in a tropical marine boundary layer. *Proceedings of the*
950 *National Academy of Sciences*, *110*(44), 17668–17673.
951 https://doi.org/10.1073/pnas.1216639110

952 Shah, V., Jaeglé, L., Thornton, J. A., Lopez-Hilfiker, F. D., Lee, B. H., Schroder, J. C., et al.
953 (2018). Chemical feedbacks weaken the wintertime response of particulate sulfate and
954 nitrate to emissions reductions over the eastern United States. *Proceedings of the National*
955 *Academy of Sciences of the United States of America*, *115*(32), 8110–8115.
956 https://doi.org/10.1073/pnas.1803295115

957 Shah, V., Jacob, D. J., Li, K., Silvern, R. F., Zhai, S., Liu, M., et al. (2020). Effect of changing
958 NOx lifetime on the seasonality and long-term trends of satellite-observed tropospheric
959 NO2 columns over China. *Atmospheric Chemistry and Physics*, *20*(3), 1483–1495.
960 https://doi.org/10.5194/acp-20-1483-2020

961 Shao, J., Chen, Q., Wang, Y., Lu, X., He, P., Sun, Y., et al. (2019). Heterogeneous sulfate
962 aerosol formation mechanisms during wintertime Chinese haze events: air quality model
963 assessment using observations of sulfate oxygen isotopes in Beijing. *Atmospheric*
964 *Chemistry and Physics*, *19*(9), 6107–6123. https://doi.org/10.5194/acp-19-6107-2019

965 Sheng, J., Zhao, D., Ding, D., Li, X., Huang, M., Gao, Y., et al. (2018). Characterizing the level,
966 photochemical reactivity, emission, and source contribution of the volatile organic
967 compounds based on PTR-TOF-MS during winter haze period in Beijing, China.
968 *Atmospheric Research*, *212*, 54–63. https://doi.org/10.1016/j.atmosres.2018.05.005

969 Sherwen, T., Evans, M. J., Sommariva, R., Hollis, L. D. J., Ball, S. M., Monks, P. S., et al.
970 (2017). Effects of halogens on European air-quality. *Faraday Discussions*, *200*, 75–100.
971 https://doi.org/10.1039/C7FD00026J

972 Shi, G., Xu, J., Shi, X., Liu, B., Bi, X., Xiao, Z., et al. (2019). Aerosol pH Dynamics During
973 Haze Periods in an Urban Environment in China: Use of Detailed, Hourly, Speciated
974 Observations to Study the Role of Ammonia Availability and Secondary Aerosol Formation
975 and Urban Environment. *Journal of Geophysical Research: Atmospheres*, *124*(16), 9730–
976 9742. https://doi.org/10.1029/2018JD029976

977 Song, C., He, J., Wu, L., Jin, T., Chen, X., Li, R., et al. (2017). Health burden attributable to
978 ambient PM2.5 in China. *Environmental Pollution*, *223*, 575–586.
979 https://doi.org/10.1016/J.ENVPOL.2017.01.060

980 Song, W., Liu, X.-Y., Wang, Y.-L., Tong, Y.-D., Bai, Z.-P., & Liu, C.-Q. (2020). Nitrogen
981 isotope differences between atmospheric nitrate and corresponding nitrogen oxides: A new
982 constraint using oxygen isotopes. *Science of The Total Environment*, *701*, 134515.
983 https://doi.org/10.1016/j.scitotenv.2019.134515

984 Sun, J., Wang, Y., Wu, F., Tang, G., Wang, L., Wang, Y., & Yang, Y. (2018). Vertical
985 characteristics of VOCs in the lower troposphere over the North China Plain during
986 pollution periods. *Environmental Pollution*, *236*, 907–915.
987 https://doi.org/10.1016/j.envpol.2017.10.051

988 Sun, Y., Lei, L., Zhou, W., Chen, C., He, Y., Sun, J., et al. (2020). A chemical cocktail during
989 the COVID-19 outbreak in Beijing, China: Insights from six-year aerosol particle

composition measurements during the Chinese New Year holiday. *Science of the Total Environment*, *742*, 140739. https://doi.org/10.1016/j.scitotenv.2020.140739

Tan, F., Tong, S., Jing, B., Hou, S., Liu, Q., Li, K., et al. (2016). Heterogeneous reactions of NO 2 with CaCO 3 –(NH 4) 2 SO 4 mixtures at different relative humidities. *Atmospheric Chemistry and Physics*, *16*(13), 8081–8093. https://doi.org/10.5194/acp-16-8081-2016

Tan, F., Jing, B., Tong, S., & Ge, M. (2017). The effects of coexisting Na2SO4 on heterogeneous uptake of NO2 on CaCO3 particles at various RHs. *Science of the Total Environment*, *586*, 930–938. https://doi.org/10.1016/j.scitotenv.2017.02.072

Tan, Z., Lu, K., Jiang, M., Su, R., Wang, H., Lou, S., et al. (2019). Daytime atmospheric oxidation capacity in four Chinese megacities during the photochemically polluted season: a case study based on box model simulation. *Atmospheric Chemistry and Physics*, *19*(6), 3493–3513. https://doi.org/10.5194/acp-19-3493-2019

Tham, Y. J., Wang, Z., Li, Q., Yun, H., Wang, W., Wang, X., et al. (2016). Significant concentrations of nitryl chloride sustained in the morning: investigations of the causes and impacts on ozone production in a polluted region of northern China. *Atmospheric Chemistry and Physics*, *16*(23), 14959–14977. https://doi.org/10.5194/acp-16-14959-2016

Thornton, J., & Abbatt, J. P. D. (2005). Measurements of HO 2 uptake to aqueous aerosol: Mass accommodation coefficients and net reactive loss. *Journal of Geophysical Research*, *110*(D8), D08309. https://doi.org/10.1029/2004JD005402

Vicars, W. C., & Savarino, J. (2014). Quantitative constraints on the 17O-excess (Δ17O) signature of surface ozone: Ambient measurements from 50°N to 50°S using the nitrite-coated filter technique. *Geochimica et Cosmochimica Acta*, *135*, 270–287. https://doi.org/10.1016/j.gca.2014.03.023

Wang, Jiaqi, Zhang, X., Guo, J., Wang, Z., & Zhang, M. (2017). Observation of nitrous acid (HONO) in Beijing, China: Seasonal variation, nocturnal formation and daytime budget. *Science of The Total Environment*, *587–588*, 350–359. https://doi.org/10.1016/j.scitotenv.2017.02.159

Wang, Junfeng, Li, J., Ye, J., Zhao, J., Wu, Y., Hu, J., et al. (2020). Fast sulfate formation from oxidation of SO2 by NO2 and HONO observed in Beijing haze. *Nature Communications*, *11*(1), 2844. https://doi.org/10.1038/s41467-020-16683-x

Wang, W., Li, X., Shao, M., Hu, M., Zeng, L., Wu, Y., & Tan, T. (2019). The impact of aerosols on photolysis frequencies and ozone production in Beijing during the 4-year period 2012–2015. *Atmospheric Chemistry and Physics*, *19*(14), 9413–9429. https://doi.org/10.5194/acp-19-9413-2019

Wang, X., Jacob, D. J., Eastham, S. D., Sulprizio, M. P., Zhu, L., Chen, Q., et al. (2019). The role of chlorine in global tropospheric chemistry. *Atmospheric Chemistry and Physics*, *19*(6), 3981–4003. https://doi.org/10.5194/acp-19-3981-2019

Wang, X., Jacob, D. J., Fu, X., Wang, T., Le Breton, M., Hallquist, M., et al. (2020). Effects of anthropogenic chlorine on PM 2.5 and ozone air quality in China. *Environmental Science & Technology*, acs.est.0c02296. https://doi.org/10.1021/acs.est.0c02296

Wang, Yan-Li, Song, W., Yang, W., Sun, X., Tong, Y., Wang, X., et al. (2019). Influences of

Atmospheric Pollution on the Contributions of Major Oxidation Pathways to PM 2.5 Nitrate Formation in Beijing. *Journal of Geophysical Research: Atmospheres*, *124*(7), 4174–4185. https://doi.org/10.1029/2019JD030284

Wang, Yuhang, Jacob, D. J., & Logan, J. A. (1998). Global simulation of tropospheric O3-NOx-hydrocarbon chemistry: 1. Model formulation. *Journal of Geophysical Research: Atmospheres*, *103*(D9), 10713–10725. https://doi.org/10.1029/98JD00158

van der Werf, G. R., Randerson, J. T., Giglio, L., van Leeuwen, T. T., Chen, Y., Rogers, B. M., et al. (2017). Global fire emissions estimates during 1997–2016. *Earth System Science Data*, *9*(2), 697–720. https://doi.org/10.5194/essd-9-697-2017

Womack, C. C., McDuffie, E. E., Edwards, P. M., Bares, R., Gouw, J. A., Docherty, K. S., et al. (2019). An Odd Oxygen Framework for Wintertime Ammonium Nitrate Aerosol Pollution in Urban Areas: NOx and VOC Control as Mitigation Strategies. *Geophysical Research Letters*, *46*(9), 4971–4979. https://doi.org/10.1029/2019GL082028

Xia, M., Wang, W., Wang, Z., Gao, J., Li, H., Liang, Y., et al. (2019). Heterogeneous uptake of N2O5 in sand dust and urban aerosols observed during the dry season in Beijing. *Atmosphere*, *10*(4), 204. https://doi.org/10.3390/ATMOS10040204

Xu, Q., Wang, S., Jiang, J., Bhattarai, N., Li, X., Chang, X., et al. (2019). Nitrate dominates the chemical composition of PM2.5 during haze event in Beijing, China. *Science of the Total Environment*, *689*, 1293–1303. https://doi.org/10.1016/j.scitotenv.2019.06.294

Yan, Y., Peng, L., Li, R., Li, Y., Li, L., & Bai, H. (2017). Concentration, ozone formation potential and source analysis of volatile organic compounds (VOCs) in a thermal power station centralized area: A study in Shuozhou, China. *Environmental Pollution*, *223*, 295–304. https://doi.org/10.1016/j.envpol.2017.01.026

Ye, C., Zhang, N., Gao, H., & Zhou, X. (2017). Photolysis of Particulate Nitrate as a Source of HONO and NOx. *Environmental Science & Technology*, *51*(12), 6849–6856. https://doi.org/10.1021/acs.est.7b00387

Yu, C., Wang, Z., Xia, M., Fu, X., Wang, W., Tham, Y. J., et al. (2020). Heterogeneous N2O5 reactions on atmospheric aerosols at four Chinese sites: improving model representation of uptake parameters. *Atmospheric Chemistry and Physics*, *20*(7), 4367–4378. https://doi.org/10.5194/acp-20-4367-2020

Yu, D., Tan, Z., Lu, K., Ma, X., Li, X., Chen, S., et al. (2020). An explicit study of local ozone budget and NOx-VOCs sensitivity in Shenzhen China. *Atmospheric Environment*, *224*, 117304. https://doi.org/10.1016/j.atmosenv.2020.117304

Zhang, B., Zhao, B., Zuo, P., Huang, Z., & Zhang, J. (2017). Ambient peroxyacyl nitrate concentration and regional transportation in Beijing. *Atmospheric Environment*, *166*, 543–550. https://doi.org/10.1016/j.atmosenv.2017.07.053

Zhang, G., Xia, L., Zang, K., Xu, W., Zhang, F., Liang, L., et al. (2020). The abundance and inter-relationship of atmospheric peroxyacetyl nitrate (PAN), peroxypropionyl nitrate (PPN), O3, and NOy during the wintertime in Beijing, China. *Science of the Total Environment*, *718*, 137388. https://doi.org/10.1016/j.scitotenv.2020.137388

Zhang, H., Xu, X., Lin, W., & Wang, Y. (2014). Wintertime peroxyacetyl nitrate (PAN) in the

megacity Beijing: Role of photochemical and meteorological processes. *Journal of Environmental Sciences (China)*, *26*(1), 83–96. https://doi.org/10.1016/S1001-0742(13)60384-8

Zhang, J., An, J., Qu, Y., Liu, X., & Chen, Y. (2019). Impacts of potential HONO sources on the concentrations of oxidants and secondary organic aerosols in the Beijing-Tianjin-Hebei region of China. *Science of The Total Environment*, *647*, 836–852. https://doi.org/10.1016/j.scitotenv.2018.08.030

Zhang, L., Gong, S., Padro, J., & Barrie, L. (2001). A size-segregated particle dry deposition scheme for an atmospheric aerosol module. *Atmospheric Environment*, *35*(3), 549–560. https://doi.org/10.1016/S1352-2310(00)00326-5

Zhang, Y.-L., & Cao, F. (2015). Fine particulate matter (PM2.5) in China at a city level. *Scientific Reports*, *5*(1), 14884. https://doi.org/10.1038/srep14884

Zheng, B., Tong, D., Li, M., Liu, F., Hong, C., Geng, G., et al. (2018). Trends in China's anthropogenic emissions since 2010 as the consequence of clean air actions. *Atmospheric Chemistry and Physics*, *18*(19), 14095–14111. https://doi.org/10.5194/acp-18-14095-2018

Zhou, W., Zhao, J., Ouyang, B., Mehra, A., Xu, W., Wang, Y., et al. (2018). Production of N2O5 and ClNO2 in summer in urban Beijing, China. *Atmospheric Chemistry and Physics*, *18*(16), 11581–11597. https://doi.org/10.5194/acp-18-11581-2018

Zhou, W., Gao, M., He, Y., Wang, Q., Xie, C., Xu, W., et al. (2019). Response of aerosol chemistry to clean air action in Beijing, China: Insights from two-year ACSM measurements and model simulations. *Environmental Pollution*, *255*, 113345. https://doi.org/10.1016/j.envpol.2019.113345

Other supporting references

Acton, W. J. F., Huang, Z., Davison, B., Drysdale, W. S., Fu, P., Hollaway, M., et al. (2020). Surface–atmosphere fluxes of volatile organic compounds in Beijing. *Atmospheric Chemistry and Physics*, *20*(23), 15101–15125. https://doi.org/10.5194/acp-20-15101-2020

Fu, X., Wang, T., Zhang, L., Li, Q., Wang, Z., Xia, M., et al. (2019). The significant contribution of HONO to secondary pollutants during a severe winter pollution event in southern China. *Atmospheric Chemistry and Physics*, *19*(1), 1–14. https://doi.org/10.5194/acp-19-1-2019

Haskins, J. D., Lopez-Hilfiker, F. D., Lee, B. H., Shah, V., Wolfe, G. M., DiGangi, J., et al. (2019). Anthropogenic Control Over Wintertime Oxidation of Atmospheric Pollutants. *Geophysical Research Letters*, *46*(24), 14826–14835. https://doi.org/10.1029/2019GL085498

Hoffmann, E. H., Tilgner, A., Vogelsberg, U., Wolke, R., & Herrmann, H. (2019). Near-Explicit Multiphase Modeling of Halogen Chemistry in a Mixed Urban and Maritime Coastal Area. *ACS Earth and Space Chemistry*, *3*(11), 2452–2471. https://doi.org/10.1021/acsearthspacechem.9b00184

Li, D., Xue, L., Wen, L., Wang, X., Chen, T., Mellouki, A., et al. (2018). Characteristics and sources of nitrous acid in an urban atmosphere of northern China: Results from 1-yr continuous observations. *Atmospheric Environment*, *182*, 296–306. https://doi.org/10.1016/J.ATMOSENV.2018.03.033

Li, J., Xie, S. D., Zeng, L. M., Li, L. Y., Li, Y. Q., & Wu, R. R. (2015). Characterization of ambient volatile organic compounds and their sources in Beijing, before, during, and after Asia-Pacific Economic Cooperation China 2014. *Atmospheric Chemistry and Physics*, *15*(14), 7945–7959. https://doi.org/10.5194/acp-15-7945-2015

Li, K., Li, J., Tong, S., Wang, W., Huang, R.-J., & Ge, M. (2019). Characteristics of wintertime VOCs in suburban and urban Beijing: concentrations, emission ratios, and festival effects. *Atmospheric Chemistry and Physics*, *19*(12), 8021–8036. https://doi.org/10.5194/acp-19-8021-2019

Li, Q., Badia, A., Wang, T., Sarwar, G., Fu, X., Zhang, L., et al. (2020). Potential Effect of Halogens on Atmospheric Oxidation and Air Quality in China. *Journal of Geophysical Research: Atmospheres*, *125*(9). https://doi.org/10.1029/2019JD032058

McCulloch, A., Aucott, M. L., Benkovitz, C. M., Graedel, T. E., Kleiman, G., Midgley, P. M., & Li, Y.-F. (1999). Global emissions of hydrogen chloride and chloromethane from coal combustion, incineration and industrial activities: Reactive Chlorine Emissions Inventory. *Journal of Geophysical Research: Atmospheres*, *104*(D7), 8391–8403. https://doi.org/10.1029/1999JD900025

Romer, P. S., Wooldridge, P. J., Crounse, J. D., Kim, M. J., Wennberg, P. O., Dibb, J. E., et al. (2018). Constraints on Aerosol Nitrate Photolysis as a Potential Source of HONO and NO x. *Environmental Science & Technology*, *52*(23), 13738–13746. https://doi.org/10.1021/acs.est.8b03861

Shi, Y., Hu, F., Xiao, Z., Fan, G., & Zhang, Z. (2020). Comparison of four different types of planetary boundary layer heights during a haze episode in Beijing. *Science of the Total Environment*, *711*, 134928. https://doi.org/10.1016/j.scitotenv.2019.134928

Su, T., Li, Z., & Kahn, R. (2018). Relationships between the planetary boundary layer height and surface pollutants derived from lidar observations over China: regional pattern and influencing factors. *Atmospheric Chemistry and Physics*, *18*(21), 15921–15935. https://doi.org/10.5194/acp-18-15921-2018

Tang, G., Zhang, J., Zhu, X., Song, T., Münkel, C., Hu, B., et al. (2016). Mixing layer height and its implications for air pollution over Beijing, China. *Atmospheric Chemistry and Physics*, *16*(4), 2459–2475. https://doi.org/10.5194/acp-16-2459-2016

1147 References From the Supporting Information
1148

1149 Acton, W. J. F., Huang, Z., Davison, B., Drysdale, W. S., Fu, P., Hollaway, M., et al. (2020).
1150 Surface–atmosphere fluxes of volatile organic compounds in Beijing. *Atmospheric*
1151 *Chemistry and Physics*, *20*(23), 15101–15125. https://doi.org/10.5194/acp-20-15101-2020

1152 Fu, X., Wang, T., Zhang, L., Li, Q., Wang, Z., Xia, M., et al. (2019). The significant contribution
1153 of HONO to secondary pollutants during a severe winter pollution event in southern China.
1154 *Atmospheric Chemistry and Physics*, *19*(1), 1–14. https://doi.org/10.5194/acp-19-1-2019

1155 Haskins, J. D., Lopez-Hilfiker, F. D., Lee, B. H., Shah, V., Wolfe, G. M., DiGangi, J., et al.
1156 (2019). Anthropogenic Control Over Wintertime Oxidation of Atmospheric Pollutants.
1157 *Geophysical Research Letters*, *46*(24), 14826–14835.
1158 https://doi.org/10.1029/2019GL085498

1159 Hoffmann, E. H., Tilgner, A., Vogelsberg, U., Wolke, R., & Herrmann, H. (2019). Near-Explicit
1160 Multiphase Modeling of Halogen Chemistry in a Mixed Urban and Maritime Coastal Area.
1161 *ACS Earth and Space Chemistry*, *3*(11), 2452–2471.
1162 https://doi.org/10.1021/acsearthspacechem.9b00184

1163 Li, D., Xue, L., Wen, L., Wang, X., Chen, T., Mellouki, A., et al. (2018). Characteristics and
1164 sources of nitrous acid in an urban atmosphere of northern China: Results from 1-yr
1165 continuous observations. *Atmospheric Environment*, *182*, 296–306.
1166 https://doi.org/10.1016/J.ATMOSENV.2018.03.033

1167 Li, J., Xie, S. D., Zeng, L. M., Li, L. Y., Li, Y. Q., & Wu, R. R. (2015). Characterization of
1168 ambient volatile organic compounds and their sources in Beijing, before, during, and after
1169 Asia-Pacific Economic Cooperation China 2014. *Atmospheric Chemistry and Physics*,
1170 *15*(14), 7945–7959. https://doi.org/10.5194/acp-15-7945-2015

1171 Li, K., Li, J., Tong, S., Wang, W., Huang, R.-J., & Ge, M. (2019). Characteristics of wintertime
1172 VOCs in suburban and urban Beijing: concentrations, emission ratios, and festival effects.
1173 *Atmospheric Chemistry and Physics*, *19*(12), 8021–8036. https://doi.org/10.5194/acp-19-
1174 8021-2019

1175 Li, Q., Badia, A., Wang, T., Sarwar, G., Fu, X., Zhang, L., et al. (2020). Potential Effect of
1176 Halogens on Atmospheric Oxidation and Air Quality in China. *Journal of Geophysical*
1177 *Research: Atmospheres*, *125*(9). https://doi.org/10.1029/2019JD032058

1178 McCulloch, A., Aucott, M. L., Benkovitz, C. M., Graedel, T. E., Kleiman, G., Midgley, P. M., &
1179 Li, Y.-F. (1999). Global emissions of hydrogen chloride and chloromethane from coal
1180 combustion, incineration and industrial activities: Reactive Chlorine Emissions Inventory.
1181 *Journal of Geophysical Research: Atmospheres*, *104*(D7), 8391–8403.
1182 https://doi.org/10.1029/1999JD900025

1183 Romer, P. S., Wooldridge, P. J., Crounse, J. D., Kim, M. J., Wennberg, P. O., Dibb, J. E., et al.
1184 (2018). Constraints on Aerosol Nitrate Photolysis as a Potential Source of HONO and NO
1185 x. *Environmental Science & Technology*, *52*(23), 13738–13746.
1186 https://doi.org/10.1021/acs.est.8b03861

1187 Shi, Y., Hu, F., Xiao, Z., Fan, G., & Zhang, Z. (2020). Comparison of four different types of
1188 planetary boundary layer heights during a haze episode in Beijing. *Science of the Total*

Environment, *711*, 134928. https://doi.org/10.1016/j.scitotenv.2019.134928

Su, T., Li, Z., & Kahn, R. (2018). Relationships between the planetary boundary layer height and surface pollutants derived from lidar observations over China: regional pattern and influencing factors. *Atmospheric Chemistry and Physics*, *18*(21), 15921–15935. https://doi.org/10.5194/acp-18-15921-2018

Tang, G., Zhang, J., Zhu, X., Song, T., Münkel, C., Hu, B., et al. (2016). Mixing layer height and its implications for air pollution over Beijing, China. *Atmospheric Chemistry and Physics*, *16*(4), 2459–2475. https://doi.org/10.5194/acp-16-2459-2016